

Development of Extrinsic Functions for Optimal Synthesis and Design—Application to Distillation-based Separation Processes

Juan I. Manassaldi¹, Miguel C. Mussati^{1,2}, Nicolás J. Scenna¹, Sergio F. Mussati^{1,2,*}

¹ CAIMI Centro de Aplicaciones Informáticas y Modelado en Ingeniería, Universidad Tecnológica Nacional, Facultad Regional Rosario, Zeballos 1346, S2000BQA Rosario, Argentina.

² INGAR Instituto de Desarrollo y Diseño (CONICET-UTN), Avellaneda 3657, S3002GJC Santa Fe, Argentina

* Corresponding author: mussati@santafe-conicet.gov.ar

Abstract

This work deals with the development and implementation of mathematical models in the General Algebraic Modeling System (GAMS) environment for optimization purposes, involving extrinsic functions that are executed outside GAMS from dynamic-link libraries (DLL) implemented in the programming language C. Three DLL libraries are developed to calculate thermodynamic properties: the Raoult's law for vapor-liquid equilibrium, the Non-Random Two-Liquid (NRTL) model, and the Peng-Robinson equation of state. A detailed description on how GAMS and DLL libraries interact is presented. Case studies dealing with the optimal design of multi-component distillation columns with increasing complexity levels are discussed. For the proposed case studies, the obtained results show that the usage of the proposed extrinsic functions allows to significantly enhance the model implementation compared to the traditional model implementation approach, and to considerably reduce the model size as well as the computational time required by the optimization algorithms.

Keywords: Mathematical Programming; Algebraic Modeling Languages; GAMS; Extrinsic Functions; External Equations; Distillation.

1. Introduction

The mathematical modeling of any chemical engineering process is a complex and challenging task because of the non-linear nature of the equations required to describe both the pieces of equipment and the process itself. Currently, algebraic modeling languages (AML), which are high-level computer programming languages, are widely employed to solve highly non-linear and large scale optimization problems, such as GAMS (General Algebraic Modeling System) (GAMS Development Corp., 2018a), AIMMS (Advanced Interactive Multidimensional Modeling System) (AIMMS B.V., 2018), AMPL (A Mathematical Programming Language) (AMPL Optimization Inc., 2018), FICO Xpress (Fair Isaac Corporation, 2018).

35 In chemical engineering, the estimation of physicochemical properties is a critical task to
36 build models to simulate and/or to optimize a production process and it is one of the main sources
37 of nonlinearities. The use of advanced physicochemical property estimation packages in algebraic
38 modeling languages generally requires defining numerous parameters, variables, and intermediate
39 equations that significantly increase the model's size (equations and variables). In addition, a
40 realistic description of reaction kinetics, vapor-liquid-equilibrium, and/or caloric properties involves
41 non-linear constraints leading to very complex models that often face convergence problems. To
42 overcome this, several authors used external routines with the main aim of transferring calculation
43 procedures to an external module (Tolsma et al., 2000, 2002; Poth et al., 2003). Tolsma et al. (2002)
44 presented source-to-source code transformation techniques to properly incorporate external code
45 into an equation-oriented process modeling environment. They employed Fortran to implement the
46 external routines and ABACUSS II (Tolsma et al., 2000) as the equation-oriented modeling
47 environment. The authors highlighted that the proposed techniques can be successfully used for
48 incorporating external procedures into modular simulators for steady-state simulation and
49 optimization.

50 External routines have been widely suggested to solve complex sub-problems in several
51 process optimizations (Kravanja and Grossmann, 1996; Noronha et al., 1997). Also, external
52 equilibrium calculations were implemented using process simulators (Caballero and Grossmann,
53 2010). Generally, the use of external modules in equation-based optimization problems exploits the
54 nature of a subset of equality constraints that are part of the feasible region, to solve the problem
55 more efficiently. This allows the use of tailored algorithms or even black-box type models.

56 In this work, GAMS (GAMS Development Corp., 2018a) is selected as the algebraic
57 modeling language not only because it is widely used in chemical process optimization problems
58 (Arias et al., 2016; Barttfeld et al., 2004, 2003; Manassaldi et al., 2016, 2014; Mores et al., 2018;
59 Mussati et al., 2008; Onishi et al., 2017) but also because it allows creating an external calculation
60 module. Besides the possibility of using in GAMS a “conventional” syntax in the model declaration
61 for manipulating data as well as for relating constraints (with different types of variables: integer,
62 binary, continuous), the GAMS Function Library Facility allows users to import functions from an
63 external library into a GAMS model. Specifically, GAMS offers the possibility of integrating
64 external functions packaged as a DLL – dynamic-link library – (if the operating system is
65 Windows) or SO – shared object – (if the operating system is Unix).

66 GAMS provides two different ways to include external modules: *external equations* and
67 *extrinsic functions* (GAMS Development Corp., 2018b), which were introduced in 1996 and 2011,
68 respectively. They differentiate in several aspects, mainly in their usage and implementation way.

69 The extrinsic functions are more intuitive to use and also easier to implement since the single
70 functions handle only the endogenous variables required for their computation and not the whole set
71 of variables that needs to be transferred simultaneously as in the case of the external equation. In
72 addition, extrinsic functions supplied by a DLL library can be used much more flexible.
73 Furthermore, they can provide first and second order derivative information and are supported by
74 NLP and MINLP solvers, while external equations provide first order derivative information only.
75 On the other side, the external equations allow for the simultaneous solution of a whole equation
76 system with dedicated algorithms, while the extrinsic functions are limited to the computation of
77 scalar values and a maximum number of arguments of 20. Lastusilta et al. (2012) presented a
78 comparative analysis between the use of external equations and extrinsic functions in several
79 optimization problems. They concluded that the usage of extrinsic functions seems to be more
80 intuitive, both options have different benefits, and there is not a clearly superior approach.

81 Several authors made the most of external equation feature in GAMS. Brusis (2003)
82 employed external equations to estimate the thermodynamic properties and the column size for
83 optimizing azeotropic distillation processes. Poth et al. (2003) further extended this approach to
84 reactive distillation processes by using external equations to describe reaction kinetics. The authors
85 concluded that the model's convergence behavior when using external equations in the model
86 building resulted in significantly improvements with a lower number of iterations than traditional
87 approach. In a similar way, Kossack et al. (2006) and Kraemer et al. (2009) addressed the optimal
88 design of distillation columns by employing external equations in GAMS to calculate the
89 thermodynamic properties (liquid activity coefficients and enthalpies) as well as the required
90 derivatives. In Kossack et al. (2006), a combination of shortcut calculations using the rectification
91 body method (RBM) and rigorous optimization is proposed. The former RBM method is used to
92 identify feasible products by minimizing the energy demand required for the separation. The
93 obtained solution is then used not only to initialize and bound the variables of the rigorous model.
94 In the same way, Skiborowski et al. (2015) recently presented an approach for the optimization-
95 based design of heterogeneous azeotropic distillation processes based on equilibrium tray models
96 and rigorous thermodynamic models, employing GAMS. In order to guarantee a correct selection of
97 the number of phases in each column tray, they proposed a phase stability test and reformulated the
98 equilibrium equations by using external equations. The authors encapsulated the whole VLE or
99 VLLE model and, therefore, performed the solution of an implicit function defined by a single or
100 more sets of nonlinear equations. Some applications on membrane-assisted distillation processes,
101 dividing wall columns, and shortcut modeling can be found in Skiborowski et al. (2018, 2014).
102 Recker et al. (2015) proposed a systematic optimization-based approach, implemented in GAMS,

103 for the design of chemical reaction-separation processes. They used external equations to calculate
104 the vapor-liquid equilibrium (VLE) of the specific analyzed case. Waltermann and Skiborowski
105 (2016) presented an efficient optimization-based method for the evaluation of different distillation
106 configurations, also implemented in GAMS. The proposed approach is based on a superstructure
107 equilibrium tray model considering rigorous thermodynamic models. Similarly to Recker et al.
108 (2015), the thermodynamic properties are calculated by means of external equations. Schilling et al.
109 (2017a, 2017b) simultaneously optimized the process and the working fluid of an Organic Rankine
110 Cycle (ORC) using the Perturbed-Chain Statistical Associating Fluid Theory (PC-SAFT) equation
111 of state for modeling the thermodynamic properties of the working fluid. The PC-SAFT and the
112 process models were linked to GAMS using external equations. A significant contribution was
113 presented by Bongarts and Mitsos (2017), who extended the use of implicit functions in the context
114 of global optimization of process flowsheets which requires not only the evaluation of function
115 values and derivative information, but also the propagation of relaxations.

116 Recently, Manassaldi (2017) proposed an optimization approach using extrinsic functions to
117 obtain the optimal configuration and operating conditions of a Combined Cycle Gas Turbine
118 (CCGT) for different target levels of electricity generation. Specifically, a DLL library with several
119 extrinsic functions was created not only to calculate the physicochemical properties of the working
120 fluids (water and combustion exhaust gas) but also to describe the behavior of the main process
121 units (gas turbine, combustor, steam turbines, among others). The extrinsic functions included in the
122 DLL libraries developed by Manassaldi (2017) can be easily extended to different case studies
123 (utility system plants and several NGCCs (Manassaldi et al., 2016, 2014), absorption refrigeration
124 cycles (Mazzei et al., 2014), among others) without modifying the source codes.

125 Based on this, it is clear the benefit of providing a set of thermodynamic packages that can
126 be included into rigorous chemical process simulation/optimization models. Thus, a main purpose
127 of this paper is to present a collection of DLL libraries implemented in the C programming
128 language to facilitate the integration of rigorous thermodynamic packages (the Raoult's law, the
129 Non-Random Two-Liquid (NRTL) model, and the Peng-Robinson equation of state) into algebraic
130 modeling languages, in particular into GAMS.

131 To the best of our knowledge, this type of integration using extrinsic functions has not been
132 reported in the literature. The DLL libraries for both simulation and optimization purposes in
133 different application fields will be available for the readers. A database with 430 components is
134 included, which allows considering many mixtures of different components.

135 This paper is organized as follows. Section 2 describes the developed DLL libraries. Section
136 3 describes the successive steps that must be executed during the DLL library loading process.

137 Section 4 introduces how the developed DLL libraries can be included in optimization
138 mathematical models. Section 5 shows the application of the proposed DLL libraries to optimize
139 distillation-based separation processes. Finally, Section 6 presents the conclusions and future works.

140 **2. Library description**

141 In this work, the capability of extrinsic functions to establish direct relationships between
142 thermodynamic properties (enthalpy, entropy, etc.) and the intensive variables (temperature,
143 pressure, and composition) of the main process streams is exploited. The three general-purpose
144 thermodynamic libraries were developed:

145 – *RaoultLaw.dll*: Ideal solution (liquid phase) + Ideal gas (vapor phase).

146 – *NRTLideal.dll*: NRTL activity coefficient (liquid phase) (Renon and Prausnitz, 1968) + Ideal gas
147 (vapor phase).

148 – *PengRobinson.dll*: Peng Robinson equation of state (both phases) (Peng and Robinson, 1976).

149 Each DLL library contains a set of different extrinsic functions and each function
150 corresponds to a thermodynamic property. All functions require temperature (K), pressure (bar),
151 and component mole fractions as input arguments. The number of extrinsic functions and the input
152 arguments of each function automatically vary according to the number of involved compounds (up
153 to 18 compounds). If n is the number of compounds, there will be $(6 + 2n)$ extrinsic functions and
154 each one will have $(n + 2)$ input arguments. For example, a binary mixture results in eight extrinsic
155 functions, each one having four input arguments.

156 For the sake of generality, all libraries contain the same extrinsic functions (Table 1) but
157 each one contains a different method to estimate the thermodynamic properties. For instance,
158 according to Table 1, the extrinsic function named as *rho_liq* returns the value of density
159 corresponding to a liquid mixture. So, if the *PengRobinson.dll* library is used, the calculation is
160 done from the compressibility factor; but if the *RaoultLaw.dll* is used, it is estimated from the
161 Hakinson-Thomson method. The estimation methods used in each DLL library are presented in
162 Appendix A (Tables A.1–A.3).

163 **Insert Table 1**

164 The thermodynamic libraries were implemented in the C programming language using
165 DevC++ (Bloodshed, 2018) as a development environment (IDE) and TDM-GCC (TDM-GCC,
166 2018) as a compiler. As mentioned, the number of functions and input arguments change with the
167 number of compounds. For a better performance, all the extrinsic functions involve analytic
168 implementations of the corresponding gradient vectors and Hessian matrixes.

169 3. DLL library loading process

170 Each DLL library was implemented in such a way to be adapted to different situations since
171 the appropriate thermodynamic estimates depend on the type of mixture to be modeled. Therefore,
172 the users must choose the most suitable available library for the mixture under study.

173 Extrinsic functions are used like any traditional mathematical function of GAMS (intrinsic
174 function). But, unlike intrinsic functions, they need to be ‘pre-loaded’ for their usage. Therefore, a
175 series of statements should be introduced at the beginning of the GAMS file. Figure 1 illustrates the
176 successive steps that must be executed during the DLL library loading process.

177 **Insert Figure 1**

178 The set of developed libraries automatically identifies the involved compounds by reading a
179 TXT file that is created by the user. For this purpose, in Step 1 the involved compounds are defined
180 in a TXT file according to their ID number in the pure compound database (Kooijman and Taylor,
181 2016). In this step, the binary interaction parameters must also be provided for the
182 *PengRobinson.dll* and *RaoultLaw.dll* libraries. To avoid identification problems, each library has an
183 assigned file name that the user must respect. More information about the creation of the TXT files
184 can be found in Manassaldi et al. (2018).

185 In Step 2 the DLL library, which contains the desired extrinsic functions to be used in the
186 GAMS model, is called. Steps 1 and 2 are included as statements at the beginning of the GAMS
187 file.

188 Steps 3 and 4 are automatically performed by the DLL library. In Step 3 the DLL library
189 reads the TXT file (that contains the compound IDs) and determines the number of involved
190 compounds in the mixture. The name of the TXT file has to be respected so that the library can
191 identify it. Once the number of compounds n is known, the number of extrinsic functions ($6 + 2n$)
192 and input arguments of each one ($2 + n$) are established. It is important to note that the libraries
193 automatically adapt to the number of compounds, so the source code must not be modified whatever
194 mixture is to be modeled (with the components included in the library). Extrinsic functions allow
195 storing information in the memory to be used during the solver execution. So, in Step 4, once all the
196 compounds are identified, the database is accessed and the parameters of each compound are stored
197 (critical properties, heat capacity polynomial constants, etc.). In addition, from the information
198 contained in the TXT file, binary interaction parameters can also be stored (if necessary).

199 In Step 5 the extrinsic functions that are going to be used in the model are defined. In this
200 step it is not necessary to include all available functions but only those of interest. This step is also
201 included as a statement within the GAMS file. Then, once the previous steps have been successfully

202 completed, the extrinsic functions are already available for their use. According to the user needs,
203 they can be employed to define parameters, initialize model variables, and/or explicitly include
204 them in equations.

205 **4. DLL library inclusion in optimization mathematical models**

206 As mentioned earlier, the model implementation using extrinsic functions allows a simple
207 and friendly inclusion of the thermodynamic package. This approach can be extended in a general
208 way to more complex processes with the higher number of variables and equations.

209 Figure 2 presents two approaches to build a chemical process mathematical model in
210 Algebraic Modeling Language software. The solid line strategy follows the classical
211 implementation way, which is hereafter named as MS1. The dotted line strategy uses the
212 thermodynamic packages implemented by extrinsic functions, which is hereafter named as MS2. As
213 is observed, both methodologies only differ on how the thermodynamic properties are modeled and
214 implemented.

215

Insert Figure 2

216 The first step in both alternatives (*Step 1*) is to define the system under study (real world);
217 for instance, it can be an entire chemical process or individual pieces of process equipment. Then, a
218 mathematical model including sets of equations and inequations is developed to describe all the
219 existing physical and chemical phenomena (*Step 2*). This step corresponds to the development of a
220 theoretical model that describes the process (or piece of equipment) under study.

221 For implementation convenience, the mathematical model was separated into two main
222 groups of equations (*Steps 3 and 4*). As is seen in *Step 3*, the first group of equations is the same in
223 both approaches. It contains the process characteristic equations, where the most frequent are, for
224 instance, the mass and energy balances, equilibrium equations, cost estimation, and process
225 restrictions.

226 The second group of equations corresponds to the calculation of thermodynamic properties
227 (thermodynamic package). As illustrated, *Step 4** (in the 'traditional' formulation) includes all the
228 equations and necessary variables for the calculation of thermodynamic properties. While *Step 4***
229 (in the proposed approach) only includes direct functions instead of a set of mathematical
230 constraints.

231 The use of extrinsic functions takes advantage of the direct relationships between
232 thermodynamic properties and main variables (T, P, and composition); this corresponds to a
233 partition of the set of constraints. As mentioned, the extrinsic functions must be pre-loaded for their
234 use following the steps described in Section 3.

235 **5. Case studies**

236 The developed DLL libraries are here employed to optimize distillation-based separation
237 processes as illustrative cases. Even though the distillation processes have been studied for decades
238 and there exist a vast amount of published papers on design, operating modes, and control
239 strategies of such processes, they offer an excellent benchmark for testing novel solution strategies
240 due to their nonlinear characteristics and the trade-offs existing among model variables (Malinen,
241 2011). Indeed, as mentioned in Section 1, several authors utilized and tested external equation in the
242 modeling of this type of separation processes (Brusis, 2003; Poth et al., 2003; Skiborowski et al.,
243 2015).

244 Figure 3 illustrates a schematic of a simple distillation column. The mixture (F) is fed at the
245 feed tray (FT), dividing the column in two main sections: a) an enriching or rectification section,
246 where volatile components are removed by contacting the rising vapor stream with the down-
247 flowing liquid stream; and b) a stripping section, where the heavier components in the liquid phase
248 are concentrated. The reboiler (REB) is a heat exchanger where a vapor stream is generated, which
249 moves up the column. The liquid stream leaving the reboiler is the bottom product (B). At the top of
250 the column, a total condenser (COND) is considered to condense the hot vapor leaving the column.
251 A fraction of the condensate is recycled back to the top of the column (reflux R) and the other
252 fraction is the top product or distillate (D).

253 **Insert Figure 3**

254 The optimal design of distillation columns involves several trade-offs among the energy
255 consumption in the reboiler, the number of distillation trays (sizing), and product specifications,
256 among others. For instance, for a given product purity, the higher number of trays (capital cost), the
257 lower reflux ratio and the lower energy consumption in the reboiler (energy cost).

258 To illustrate the usage of the DLL libraries, two case studies consisting on the optimization
259 of distillation columns with different complexity levels are presented. These case studies were
260 selected as examples of classical modeling problems to show the modeling strategy here presented
261 and its performance. Here, the focus is mainly on the modeling task following the guidelines
262 provided above (Figure 2).

263 **5.1 Case study 1**

264 The case study 1 consists in separating by means of distillation an ethanol-water mixture
265 into pure water and a mixture at the azeotropic conditions.

266 The optimization problem can be stated as follows.

267 Given a mixture of 1000 kmol/h of ethanol (A) and 1000 kmol/h of water (B) at atmospheric
 268 pressure (saturated condition) and the following target specifications: a minimum water separation
 269 of 60% with a bottom product purity of 99%, the problem is to determine the optimal number of
 270 column trays, the feed tray location, the heat transfer areas of the condenser and reboiler and their
 271 corresponding heat loads, by minimization of the total annual cost, which is calculated in terms of
 272 the annualized investments and annual operating costs.

273 To this end, a superstructure-based model similar to that proposed by (Yeomans and
 274 Grossmann (2000) is used (Figure 4a). For this case study, the superstructure considers a minimum
 275 of ten existing (or fixed) stages (from $s10$ to $s19$), i.e. they always will be part of the optimal
 276 solution and will not be removed. The only reason to fix this minimum number of trays is to reduce
 277 the number of binary variables involved, and thus to reduce the calculation time.

278 **Insert Figure 4 (4a and 4b)**

279 As shown in Figure 4a, the proposed superstructure contains a maximum number of 20
 280 trays, of which 8 ($s2$ to $s9$) are modeled as conditional trays (Figure 4b). This means that, depending
 281 on the optimization criterion, all or some of these trays can be removed by the optimization
 282 algorithm. Similar to the remaining trays ($s10$ to $s19$), the condenser ($s1$) and the reboiler ($s20$) are
 283 assumed as existing trays. In addition, the trays $s2$ to $s19$ are ‘candidate’ to be the feeding tray.

284 For modeling purpose, the following three main assumptions are considered: a) vapor phase
 285 behaves ideally, b) the NRTL model is appropriate for estimating the liquid phase activity
 286 coefficients (*NRTLideal.dll* library), and c) the separation takes place at atmospheric pressure.

287 By applying the methodology proposed in Section 4, the equations corresponding to the
 288 process (Step 3 in Fig. 2) and the set of constraints that correspond to the physicochemical package
 289 (Step 4 in Fig. 2) are presented next.

290 Equation (1) corresponds to the component mass balances in the condenser (stage $s1$). L , V ,
 291 and D refer to the liquid, vapor, and distillate molar flow rates, respectively; x and y refer to the
 292 liquid and vapor phase molar fractions, respectively. s refers to the column stages ($s = s1$ to $s20$)
 293 and i to the components (A and B). The subset $COND(s)$ represents the condenser stage ($s1$).

$$294 \quad V_{s+1}y_{s+1,i} = (L_s + D)x_{s,i} \quad \forall i; \forall s / s \in COND(s) \quad (1)$$

295 The energy balance is given by Eq. (2):

$$296 \quad V_{s+1}H_{s+1}^v = Q^{cond} + (L_s + D)H_s^l \quad \forall s / s \in COND(s) \quad (2)$$

297 where Q^{cond} refers to the heat duty in the condenser, and H^l and H^v to the enthalpy of the liquid and
 298 vapor phases, respectively.

299 Equations (3) and (4) are the mass and energy balances in the reboiler (stage $s20$),
 300 respectively:

$$301 \quad L_{s-1}x_{s-1,i} = V_s y_{s,i} + L_s x_{s,i} \quad \forall i; \forall s / s \in REB(s) \quad (3)$$

$$302 \quad L_{s-1}H_{s-1}^l + Q^{reb} = V_s H_s^v + L_s H_s^l \quad \forall s / s \in REB(s) \quad (4)$$

303 where Q^{reb} refers to the heat duty required in the reboiler. The subset $REB(s)$ represents the reboiler
 304 stage ($s20$).

305 The feed stream (F_s) can be placed in one of the intermediate stages. Equations (5) and (6)
 306 are the corresponding mass and energy balances. The subset $TRAY(s)$ includes all intermediate
 307 stages ($s2$ to $s19$).

$$308 \quad F_s x_{f,i} + L_{s-1}x_{s-1,i} + V_{s+1}y_{s+1,i} = V_s y_{s,i} + L_s x_{s,i} \quad \forall i; \forall s / s \in TRAY(s) \quad (5)$$

$$309 \quad F_s H_f + L_{s-1}H_{s-1}^l + V_{s+1}H_{s+1}^v = V_s H_s^v + L_s H_s^l \quad \forall i; \forall s / s \in TRAY(s) \quad (6)$$

310 where $x_{f,i}$ and H_f are model parameters and they refer to the composition and enthalpy of the main
 311 feed stream, respectively. The mass balance in the splitter that distributes the main feed stream to
 312 the candidate feed trays is given by Eq. (7):

$$313 \quad LF = \sum_{s \in TRAY(s)} F_s \quad (7)$$

314 The following composition constraints are imposed to the liquid and vapor phases (Eq. (8)
 315 and (9), respectively):

$$316 \quad \sum_i x_{s,i} = 1 \quad \forall s \quad (8)$$

$$317 \quad \sum_i y_{s,i} = 1 \quad \forall s \quad (9)$$

318 As mentioned, the objective of this process is to separate the water content of the feed
 319 stream to increase the ethanol concentration in the distillate stream. So, a minimum water purity of
 320 0.99 in the bottom product and a separation of the inlet water content higher than 60% are imposed
 321 through Eq. (10) and (11), respectively:

$$322 \quad x_{s,A} \geq 0.99 \quad \forall s / s \in REB(s) \quad (10)$$

$$323 \quad L_s x_{s,A} \geq 0.6LF x_{l,A} \quad \forall s / s \in REB(s) \quad (11)$$

324 Discrete variables are used to model the presence or absence of trays. As shown in Fig. 4a
 325 and 4b, series of conditional trays ($NOFIXED(s)$) and fixed trays ($FIXED(s)$) are proposed.

326 In each fixed stage (condenser, reboiler, and fixed trays), the liquid and vapor phases are in
 327 equilibrium. Therefore, the fugacity of the component i in the liquid phase ($fug_{s,i}^l$) must be equal to
 328 the fugacity of the same component in the vapor phase ($fug_{s,i}^v$) (Eq. 12):

$$329 \quad fug_{s,i}^l = fug_{s,i}^v \quad \forall i; \forall s / s \in (FIXED(s) \cup COND(s) \cup REB(s)) \quad (12)$$

330 In the same way, since both phases (liquid and vapor) are in equilibrium, their temperatures
 331 are the same (Eq. 13):

$$332 \quad T_s^l = T_s^v \quad \forall s / s \in (FIXED(s) \cup COND(s) \cup REB(s)) \quad (13)$$

333 The diameter of a tray (TD) is calculated as follows:

$$334 \quad TD_s^2 = 0.77072 V_s \sqrt{(\sum y_{s,i} MW_i) / \rho_s^v} \quad \forall s / s \in TRAY(s) \quad (14)$$

335 where MW is the component molecular weight and ρ^v the vapor molar density. Then, the column
 336 diameter (CD) must be equal to or greater than the diameter of each tray (Eq. 15):

$$337 \quad CD \geq TD_s \quad \forall s / s \in TRAY(s) \quad (15)$$

338 The Boolean variable N_s in Eq. 16 defines the existence of a candidate tray in the optimal
 339 solution. If N_s is true the tray s is selected and the vapor-liquid equilibrium equations are
 340 considered. Otherwise, if N_s is false the tray is removed; so, feeding is forbidden and the liquid
 341 phase pass through the stage without any change in composition and temperature. Thus, if a tray is
 342 removed no mass transfer takes place.

$$343 \quad \left[\begin{array}{c} N_s \\ fug_{s,i}^l = fug_{s,i}^v \quad \forall i \\ T_s^l = T_s^v \end{array} \right] \vee \left[\begin{array}{c} \neg N_s \\ x_{s,i} = x_{s-1,i} \quad \forall i \\ L_s = L_{s-1} \\ T_s^l = T_{s-1}^l \\ F_s = 0 \end{array} \right] \quad \forall s / s \in NOFIXED(s) \quad (16)$$

344 The total number of trays (NT) is the sum of both fixed and candidate trays (Eq. 17):

$$345 \quad NT = \sum_{s \in FIXED(s)} 1 + \sum_{s \in NOFIXED(s)} n_s \quad (17)$$

346 where n_s is the binary variable associated to the Boolean variable N_s .

347 The objective function consists in minimizing the total annual cost (TAC), which accounts
 348 for the annualized capital expenditure ($annCAPEX$) and the operating expenditure ($OPEX$):

$$349 \quad TAC = annCAPEX + OPEX \quad (18)$$

350 The *annCAPEX* takes into account the cost for column tray (C_{tray}), column shell (C_{shell}),
 351 condenser (C_{cond}), and reboiler (C_{reb}), which are calculated as follows (in \$/year):

$$352 \quad C_{shell} = 3458.9 \cdot NT \cdot CD_{col}^{1.066} \cdot H_{tray}^{0.802} \quad (19)$$

$$353 \quad C_{tray} = 430.45 \cdot NT \cdot CD^{1.55} H_{tray} \quad (20)$$

$$354 \quad C_{reb} = 167.97 (Q^{reb})^{0.65} \quad (21)$$

$$355 \quad C_{cond} = 446.51 (Q^{cond})^{0.65} \quad (22)$$

356 where H_{tray} is the tray height.

357 The *OPEX* is calculated in terms of the cooling and steam utility costs (Eq. 23):

$$358 \quad OPEX = C_{steam} \cdot M_{steam} + C_{cw} \cdot M_{cw} \quad (23)$$

359 where M_{steam} and M_{cw} are the requirements of steam and cooling water, respectively, expressed in
 360 t/year. The associated specific costs are $C_{steam}=10.02$ \$/t and $C_{cw}=0.09$ \$/t.

361 After defining the process's characteristic equations (Eq. (1) to (23)), it is required to select
 362 the thermodynamic packages to be used. As explained in Section 4, two implementation ways of the
 363 thermodynamic packages are considered (Table 2). The former implements all thermodynamic
 364 equations in the traditional way (MS1). While the second strategy involves extrinsic functions from
 365 the *NRTLideal.dll* library (MS2). As indicated in Table 3, both ways are coupled with Eq. (1) to
 366 (23).

367 It is observed in Table 2 that Eq. (24) to (27) in MS1 and Eq. (28) to (31) in MS2 are used to
 368 calculate the thermodynamic properties (fugacities and enthalpies) required for mass and energy
 369 balances and equilibrium equations.

370 In MS1 alternative, the activity coefficient (γ), saturation pressure (P^{sat}), and pointing factor
 371 ($po\gamma$) are needed to estimate the liquid phase component fugacity (Eq. (24)). On the other hand, the
 372 ideal gas enthalpy of pure component (H^{IG}), heat of vaporization of pure component (ΔH^{vap}), and
 373 component excess enthalpy (ΔH^{ex}) are needed to estimate the liquid and vapor phase enthalpies
 374 (Eq. (26) and (27)). Equations (B.1) to (B.22) in Appendix B are necessary to calculate all
 375 mentioned variables involved in Eq. (24) to (27).

376 **Insert Table 2**

377 When extrinsic functions are employed (MS2), the main set of the thermodynamic equations
 378 express the direct relationship between the desired property (fugacity and enthalpy) and the main
 379 process stream variables (temperature, pressure, and composition). Thus, the optimization problems
 380 can be mathematically expressed as is shown in Table 3:

381 **Insert Table 3**

382 Both problems were implemented in GAMS. The discrete decisions used to select the
383 number of trays lead to mixed-integer nonlinear programming (MINLP) models, which are solved
384 using the standard Branch and Bound algorithm (SBB) as MINLP solver and CONOPT as
385 nonlinear programming (NLP) solver for the intermediate nodes. Table 4 compares the model sizes,
386 CPU times, number of iterations, number of explored nodes, and the corresponding total annual
387 cost.

388 **Insert Table 4**

389 Table 4 shows considerable differences in the model sizes. When the DLL library is used
390 (MS2 implementation), the number of equations is reduced by 68% (from 1478 to 477) and the
391 continuous variables by 73% (from 1375 to 374) when compared to the traditional strategy MS1.
392 The computation time for both models is low; however, when the extrinsic functions are used, the
393 time is reduced by 42% (from 4.137 s to 2.396 s). The number of iterations required by the MS1
394 implementation is 30% less than by the MS2 implementation (826 vs. 1139). Both models obtained
395 the same optimal solution, which is presented in Fig. 5.

396 **Insert Figure 5**

397 The optimal solution consists on a distillation column with 12 trays (6 trays were removed)
398 that is fed 5 stages above the reboiler (at $s=15$), with a reflux ratio of 0.3883 and a bottom product
399 flow rate of 606.06 kmol/h.

400 In order to verify the obtained results, the optimal solution was compared with solutions
401 obtained from several process simulators. To this end, the degrees of freedom of the simulated
402 distillation column were fixed using the optimal output values obtained by the GAMS model. Table
403 5 compares the average differences obtained in each case.

404 **Insert Table 5**

405 As shown, the MINLP output values are in agreement with those obtained with process
406 simulators. The very small differences – 0.493% in the worst case – are mainly due to the pure
407 compound database incorporated in each process simulator and some model assumptions.

408 **5.2 Case study 2**

409 The mathematical model used in the previous case study was properly extended to solve the
410 process configuration consisting of two coupled distillation columns (Fig. 6) to treat a mixture
411 consisting of three components. Both columns are coupled by means of stream mixers and splitters.
412 Similarly to the case study 1, the number of fixed trays in both columns was appropriately selected
413 to reduce the model size.

414 **Insert Figure 6**

415 Precisely, a saturated liquid mixture of n-pentane (A), n-hexane (B), and n-heptane (C) is
416 fed at a flow rate of 26 kmol/s with a molar fraction of A, B, and C of 0.33, 0.33, and 0.34,
417 respectively. A product purity of 0.98 and a minimum recovery of 98% are specified for the three
418 components. The separation takes place at atmospheric pressure. Based on the mixture type, the
419 Peng-Robinson EOS is used to estimate the thermodynamic properties. Therefore, the
420 *PengRobinson.dll* library is selected.

421 The optimization problem is similar to the previous one but with increased complexity from
422 the computational cost point of view since it involves a higher number of trade-offs and,
423 consequently, the number of variables and equations significantly increases accordingly. The
424 following discrete and continuous decisions are provided as a result of the optimization model (Fig.
425 7):

- 426 – Number of trays in each column.
- 427 – Feed tray location of each column.
- 428 – Operation parameters (operation conditions) of each column.
- 429 – Distillation sequence (for example: AB|C and A|B).
- 430 – Total annual cost of the distillation sequence.
- 431 – Heat transfer area required by the condenser and reboiler of each column.

432 Also, a comparison of the performance between both MS1 and MS2 modeling strategies is
433 presented in Table 6.

434

Insert Table 6

435 As is seen in Table 6, a significant reduction in the model size is obtained when the DLL
436 library is used, which is by 75% in the number of equations (from 5910 to 1510) and 78% in the
437 number of variables (from 5345 to 1145). The CPU time is reduced by more than half. Both
438 strategies obtained the same solution (Fig. 7), with a total annual cost of 153410 \$/year (Table 6).

439 As shown in Fig. 7, the optimal solution results in the following simple distillation
440 sequence: the main feed stream is sent to the first column where the first component is separated
441 (A|BC). The bottom product of the first column is sent to the second one where the remaining
442 components are separated (B|C).

443

Insert Figure 7

5.3 Comparison of solutions obtained using external equations and extrinsic functions.

444 Finally, a comparison of the performance between the DLL libraries using extrinsic
445 functions here developed and using external equations employed by other authors is performed
446 through another example of distillation. A GAMS model code implemented by the research group
447

448 in Process Systems Engineering AVT.PT–RWTH Aachen University (Aachener Verfahrenstechnik,
449 2019a) that employs a set of external equations is used for comparison purpose. The whole VLE or
450 VLLE model is encapsulated in the GAMS code. The source code of the external equations is
451 available for download and must be compiled by the user to create the corresponding DLL libraries.
452 To perform the comparison, the GAMS model was downloaded from the published software
453 collection (Aachener Verfahrenstechnik, 2019b) and the external equations were properly replaced
454 by the proposed extrinsic functions, retaining the constraints associated to the mass and energy
455 balances. The replacement of the external equations can be easily carried out due to the friendly
456 implementation of the GAMS model performed by the authors.

457 Similarly to the previous case studies, the optimization problem consists in determining the
458 optimal number of stages, the feed tray location, sizes, and operating conditions of the distillation
459 column that minimize the total annual cost. The main design specifications are the following:

- 460 – The column can involve a maximum number of 80 stages. The model will determine the optimal
461 number of stages.
- 462 – The feed stream is a mixture of methanol and ethanol at a molar flow rate of 50 kmol/s each, at
463 1.01325 bar (saturated condition).
- 464 – Purity specifications at the top and bottom streams are 0.995 and 0.0001 mole fraction of
465 methanol, respectively.

466 Table 7 compares the results corresponding to both solutions.

467 **Insert Table 7**

468 As shown, the values of the objective functions differ only in about 2.5% (154647.6 €/year
469 vs. 158532.2 €/year). The configuration and the column size are also similar. The small differences
470 are due to the different theoretical models used to calculate the vapor-liquid equilibrium. The
471 Wilson's method (a theoretical model based on activity coefficients) is used in the original model
472 (Aachener Verfahrenstechnik, 2019b) and the NRTL method (*NRTLideal.dll*) in the current model.
473 The computing time required by the usage of extrinsic functions is lower than of external equations
474 but the number of iterations is slightly higher.

475 As mentioned, the external equations used in the original model from Aachener
476 Verfahrenstechnik (2019b) to calculate the thermodynamic properties were replaced by those
477 presented in this paper. Since no new variables were added to the model the number of variables is
478 the same in both models, as shown in Table 7. However, the number of equations in the current
479 model is lower than the original one. This is because the original libraries require $n+3$ equations (n
480 is the number of components) for each equilibrium stage while the current libraries require $n+2$

481 equations. For this reason, the difference in the number of equations is equal to the number of
482 stages (80).

483 In the original model, a series of intermediate models are previously solved to obtain a
484 feasible initialization of the principal model. The model proposed in this paper (using extrinsic
485 functions) solves the same intermediate problems but the computation times were enhanced in all
486 cases (results not shown).

487 **5. Conclusion**

488 Different dynamic-link libraries with extrinsic functions for GAMS have been developed
489 and implemented for the calculation of thermodynamic properties according to different theoretical
490 approaches. Specifically, libraries for the Raoult's Law (*Raoultlaw.dll*), the Peng-Robinson
491 equation of state (*PenRobinson.dll*), and the Non-Random Two-Liquid model (*NRTLideal.dll*) were
492 developed.

493 Two case studies with different complexity levels were presented to illustrate the
494 performance of the libraries. The first case study dealt with the optimal synthesis and design of a
495 simple distillation column and the second one of a three-component simple distillation sequence.
496 Both cases were compared with a traditional implementation of a model including the
497 corresponding thermodynamic package. The results showed a significant decrease in both the model
498 size and computation time. This decrease was also pointed out by Poth et al. (2003) and
499 Skiborowski et al. (2015), who improved the convergence of GAMS models by employing external
500 equations, transferring complex calculations to external modules.

501 In this work, the generalization of physicochemical packages (libraries) was possible by
502 using extrinsic functions. The developed libraries can be easily included in mass and energy
503 balances of different process-units. Due to their generality, they can be easily applied to simulate
504 and/or optimize any type of chemical processes. It is clear that the use of the introduced libraries
505 based on extrinsic functions to calculate physicochemical properties greatly facilitates the modeling
506 task. In our opinion, this is the main contribution of the paper.

507 The files with the developed DLL libraries are available in the contributed software section
508 of the GAMS website (GAMS Development Corp., 2018c).

509 In future works, DLL libraries for (a) the UNiversal QUAsi-Chemical (UNIQUAC) activity
510 model, (b) the Wilson's activity model, (c) the Soave-Redlich-Kwong (SRK) equation of state, (d)
511 the modified Benedict-Webb-Rubin (mBWR) equation of state, and (e) the Perturbed-Chain
512 Statistical Associating Fluid Theory (PC-SAFT) equation of state will be also developed and

513 available to users. Also, the convenience of using extrinsic functions over embedding the
514 thermodynamic models in an external equation will be investigated.

515 Another challenge is the creation of external modules for process equipment representation.
516 The use of external functions will facilitate the implementation of conventional models (equation-
517 oriented models) or non-conventional models (black-box or neural-type models) in mathematical
518 optimization problems.

519 These challenges will be applied to our previous models such as integrated combined cycles
520 and CO₂ capture plants (Mores et al., 2018), seawater desalination processes including single
521 purpose plants (Mussati et al., 2003b, 2001) as well as dual purpose plants (Mussati et al., 2005,
522 2004, 2003a), among others.

523

524 **Acknowledgements**

525 The financial support from the Consejo Nacional de Investigaciones Científicas y Técnicas
526 (CONICET) and the Facultad Regional Rosario of the Universidad Tecnológica Nacional from
527 Argentina are gratefully acknowledged.

528 **Appendix A. Thermodynamic property estimation methods**

529 Tables A.1 and A.2 show the methods for estimating thermodynamic properties
530 implemented in each extrinsic function according to the different developed libraries. As
531 mentioned, all the libraries contain the same extrinsic functions but they differ in the used
532 theoretical model. More information about the theoretical models implemented in this article can be
533 found in Poling et al. (2001).

534

Insert Table A.1

535

Insert Table A.2

536 As can be noted in Tables A.1 and A.2, the only difference between the *NRTLideal.dll* and
537 *RaoultLaw.dll* libraries is that the latter assumes that the liquid phase behaves ideally. That is,
538 *RaoultLaw.dll* assumes a unitary activity coefficient and a unitary poynting factor, and neglects the
539 enthalpy and entropy excesses. All the extrinsic functions included in the *NRTLideal.dll* and
540 *Raoultlaw.dll* libraries follow a direct calculation sequence. That is, once the input values for the
541 extrinsic functions (e.g. pressure, temperature, and component composition) are provided, no
542 iterative process is needed to calculate the output value (e.g. enthalpy).

543 Unlike the two previous DLL libraries, the *PengRobinson.dll* library has an intermediate
544 iterative resolution process. The cubic equation of state is solved iteratively within the external
545 calculation routine. The implemented sequence uses a specific strategy for solving cubic equations

546 of state, as proposed by Deiters and Macías-Salinas (2014). In case of not being able to find the root
 547 of the cubic polynomial an error is reported and the GAMS solver ends the process. Table A.3 lists
 548 the extrinsic functions involved in the *PengRobinson.dll* library.

549 **Insert Table A.3**

550 As illustration, extracts of the source codes for computing the gradient vector and Hessian
 551 matrix in the extrinsic function corresponding to the liquid enthalpy in the Peng-Robinson library
 552 (*PengRobinson.DLL*) are provided in the supplementary material associated to this work.

553 All the developed libraries have the same pure compound database. All parameters and
 554 mathematical functions corresponding to the thermodynamic properties of the pure compounds
 555 were extracted from the Chemsep 7.15 database (Kooijman and Taylor, 2016) and are presented in
 556 Table A.4.

557 **Insert Table A.4**

558 Appendix B. NRTL equations

559 Equations (B.1) to (B.22) are related to the MS1 strategy presented in the Case Study 1.
 560 They correspond to the NRTL activity coefficient model and enthalpy estimation. A detailed
 561 theoretical description of Eq. (B.1) to (B.22) can be found in Poling et al. (2001).

$$562 \log(P_{s,i}^{sat}) = A_i + \frac{B_i}{T_s^l} + C_i \log(T_s^l) + D_i (T_s^l)^{E_i} \quad \forall s; \forall i \quad (\text{B.1})$$

$$563 Tr_{s,i} = T_s^l / Tc_i \quad \forall s; \forall i \quad (\text{B.2})$$

$$564 V_{s,i}^{(0)} = 1 + a(1 - Tr_{s,i})^{\frac{1}{3}} + b(1 - Tr_{s,i})^{\frac{2}{3}} + c(1 - Tr_{s,i}) + d(1 - Tr_{s,i})^{\frac{4}{3}} \quad \forall s; \forall i \quad (\text{B.3})$$

$$565 V_{s,i}^{(\delta)} = (e + fTr_{s,i} + gTr_{s,i}^2 + hTr_{s,i}^3) / (Tr_{s,i} - 1.00001) \quad \forall s; \forall i \quad (\text{B.4})$$

$$566 V_{s,i} = V_i^* V_{s,i}^{(0)} [1 - \omega_{SRK,i} V_{s,i}^{(\delta)}] \quad \forall s; \forall i \quad (\text{B.5})$$

$$567 poy_{s,i} = (V_{s,i} \exp(P_s - P_{s,i}^{sat})) / (RT_s^l) \quad \forall s; \forall i \quad (\text{B.6})$$

$$568 \tau_{s,i,j} = a_{i,j} / (RT_s^l) \quad \forall s; \forall i; \forall j \quad (\text{B.7})$$

$$569 G_{s,i,j} = \exp(-\alpha_{i,j} \tau_{s,i,j}) \quad \forall s; \forall i; \forall j \quad (\text{B.8})$$

$$570 S_{s,i} = \sum_{j=1}^n x_{s,j} G_{s,j,i} \quad \forall s; \forall i \quad (\text{B.9})$$

$$571 C_{s,i} = \sum_{j=1}^n x_{s,j} G_{s,j,i} \tau_{s,j,i} \quad \forall s; \forall i \quad (\text{B.10})$$

$$572 \log \gamma_{s,i} = \frac{C_{s,i}}{S_{s,i}} + \sum_{k=1}^n x_{s,k} G_{s,i,k} \left(\frac{\tau_{s,i,k}}{S_{s,k}} - \frac{C_{s,k}}{S_{s,k}^2} \right) \quad \forall s; \forall i \quad (\text{B.11})$$

$$573 \Delta H_{s,i}^{vap} = A_i (1 - Tr_{s,i})^{B_i + C_i Tr_{s,i} + D_i Tr_{s,i}^2 + C_i Tr_{s,i}^3} \quad \forall s; \forall i \quad (\text{B.12})$$

$$574 \quad \left(\frac{\partial \tau}{\partial T}\right)_{s,i,j} = -a_{i,j} / \left(R(T_s^l)^2\right) \quad \forall s; \forall i; \forall j \quad (\text{B.13})$$

$$575 \quad \left(\frac{\partial G}{\partial T}\right)_{s,i,j} = -\alpha_{i,j} G_{s,i,j} \left(\frac{\partial \tau}{\partial T}\right)_{s,i,j} \quad \forall s; \forall i; \forall j \quad (\text{B.14})$$

$$576 \quad \left(\frac{\partial S}{\partial T}\right)_{s,i} = \sum_{j=1}^n x_{s,j} \left(\frac{\partial G}{\partial T}\right)_{s,j,i} \quad \forall s; \forall i \quad (\text{B.15})$$

$$577 \quad \left(\frac{\partial C}{\partial T}\right)_{s,i} = \sum_{j=1}^n x_{s,j} \left(\left(\frac{\partial G}{\partial T}\right)_{s,j,i} \tau_{s,j,i} + G_{s,j,i} \left(\frac{\partial \tau}{\partial T}\right)_{s,j,i} \right) \quad \forall s; \forall i \quad (\text{B.16})$$

$$578 \quad M1_{s,i} = \sum_{k=1}^n x_{s,k} \left(\left(\frac{\partial G}{\partial T}\right)_{s,i,k} \tau_{s,i,k} + G_{s,i,k} \left(\frac{\partial \tau}{\partial T}\right)_{s,i,k} \right) / S_{s,k} \quad \forall s; \forall i \quad (\text{B.17})$$

$$579 \quad M2_{s,i} = \sum_{k=1}^n -x_{s,k} \left(\left(\frac{\partial G}{\partial T}\right)_{s,i,k} C_{s,k} + G_{s,i,k} \left(\frac{\partial C}{\partial T}\right)_{s,k} + G_{s,i,k} \tau_{s,i,k} \left(\frac{\partial S}{\partial T}\right)_{s,k} \right) / (S_{s,k})^2 \quad \forall s; \forall i \quad (\text{B.18})$$

$$580 \quad M3_{s,i} = \sum_{k=1}^n 2x_{s,k} G_{s,i,k} C_{s,k} \left(\frac{\partial S}{\partial T}\right)_{s,k} / (S_{s,k})^3 \quad \forall s; \forall i \quad (\text{B.19})$$

$$581 \quad \left(\frac{\partial \log \gamma}{\partial T}\right)_{s,i} = \left(\frac{\partial C}{\partial T}\right)_{s,i} \frac{1}{S_{s,i}} - \left(\frac{\partial S}{\partial T}\right)_{s,i} \frac{C_{s,i}}{S_{s,i}^2} + M1_{s,i} + M2_{s,i} + M3_{s,i} \quad \forall s; \forall i \quad (\text{B.20})$$

$$582 \quad \Delta H_{s,i}^{ex} = -R(T_s^l)^2 \left(\frac{\partial \log \gamma}{\partial T}\right)_{s,i} \quad \forall s; \forall i \quad (\text{B.21})$$

$$583 \quad H_{s,i}^{p,IG} = \Delta H_{i,f}^0 + \int_{298.15}^{T_s^p} c_{p_i}^{IG} dT \quad \forall s; \forall i; \forall p \quad (\text{B.22})$$

584 References

- 585 Aachener Verfahrenstechnik, 2019a. Process Systems Engineering (PT) - RWTH AACHEN
586 UNIVERSITY Aachener Verfahrenstechnik. <http://www.avt.rwth-aachen.de/go/id/ioaf/lidx/1>
587 (accessed 23 January 2019).
- 588 Aachener Verfahrenstechnik, 2019b. Process synthesis software collection download area.
589 [http://www.avt.rwth-aachen.de/cms/AVT/Forschung/Software/Softwaresammlung-
590 Prozesssynthese/~ipyh/Downloadbereich/?lidx=1](http://www.avt.rwth-aachen.de/cms/AVT/Forschung/Software/Softwaresammlung-Prozesssynthese/~ipyh/Downloadbereich/?lidx=1) (accessed 23 January 2019).
- 591 AIMMS B.V., 2018. Advanced Interactive Multidimensional Modeling System (AIMMS).
592 <https://www.AIMMS.com> (accessed 7 January 2019).
- 593 AMPL Optimization Inc., 2018. A Mathematical Programming Language (AMPL).
594 <https://ampl.com/> (accessed 7 January 2019).
- 595 Arias, A.M., Mussati, M.C., Mores, P.L., Scenna, N.J., Caballero, J.A., Mussati, S.F., 2016.
596 Optimization of multi-stage membrane systems for CO2 capture from flue gas. *Int. J. Greenh. Gas*
597 *Control* 53, 371–390. <https://doi.org/10.1016/j.ijggc.2016.08.005>
- 598 Bartfeld, M., Aguirre, P.A., Grossmann, I.E., 2004. A decomposition method for synthesizing
599 complex column configurations using tray-by-tray GDP models. *Comput. Chem. Eng.* 28, 2165–
600 2188. <https://doi.org/10.1016/j.compchemeng.2004.03.006>
- 601 Bartfeld, M., Aguirre, P.A., Grossmann, I.E., 2003. Alternative representations and formulations
602 for the economic optimization of multicomponent distillation columns. *Comput. Chem. Eng.* 27,
603 363–383. [https://doi.org/10.1016/S0098-1354\(02\)00213-2](https://doi.org/10.1016/S0098-1354(02)00213-2)

604 Bloodshed, 2018. Dev-C++. <https://www.bloodshed.net/devcpp.html> (accessed 7 January 2019).

605 Bongartz, D., Mitsos, A., 2017. Deterministic global optimization of process flowsheets in a
606 reduced space using McCormick relaxations. *J. Glob. Optim.* 69, 761–796.
607 <https://doi.org/10.1007/s10898-017-0547-4>

608 Brusis, D., 2003. Synthesis and optimisation of distillation processes with MINLP techniques.
609 München, Techn. Univ., Diss.

610 Caballero, J.A., Grossmann, I.E., 2010. Hybrid Simulation-Optimization Algorithms for Distillation
611 Design, in: Pierucci, S., Ferraris, G.B. (Eds.), *Computer Aided Chemical Engineering, 20 European*
612 *Symposium on Computer Aided Process Engineering*. Elsevier, pp. 637–642.
613 [https://doi.org/10.1016/S1570-7946\(10\)28107-5](https://doi.org/10.1016/S1570-7946(10)28107-5)

614 Deiters, U.K., Macías-Salinas, R., 2014. Calculation of Densities from Cubic Equations of State:
615 Revisited. *Ind. Eng. Chem. Res.* 53, 2529–2536. <https://doi.org/10.1021/ie4038664>

616 Fair Isaac Corporation, 2018. FICO® Xpress Optimization. [https://www.fico.com/en/products/fico-](https://www.fico.com/en/products/fico-xpress-optimization)
617 [xpress-optimization](https://www.fico.com/en/products/fico-xpress-optimization) (accessed 7 January 2019).

618 GAMS Development Corp., 2018a. General Algebraic Modeling System (GAMS).
619 <https://www.gams.com/> (accessed 7 January 2019).

620 GAMS Development Corp., 2018b. The GAMS User’s Guide.
621 https://www.gams.com/latest/docs/UG_MAIN.html (accessed 7 January 2019).

622 GAMS Development Corp., 2018c. GAMS - Contributed Software.
623 <https://www.gams.com/community/contributed-software/> (accessed 7 January 2019).

624 Kooijman, H., Taylor, R., 2016. ChemSep v7.15 pure component data.

625 Kossack, S., Kraemer, K., Marquardt, W., 2006. Efficient Optimization-Based Design of
626 Distillation Columns for Homogenous Azeotropic Mixtures. *Ind. Eng. Chem. Res.* 45, 8492–8502.
627 <https://doi.org/10.1021/ie060117h>

628 Kraemer, K., Kossack, S., Marquardt, W., 2009. Efficient Optimization-Based Design of
629 Distillation Processes for Homogeneous Azeotropic Mixtures. *Ind. Eng. Chem. Res.* 48, 6749–
630 6764. <https://doi.org/10.1021/ie900143e>

631 Kravanja, Z., Grossmann, I.E., 1996. A Computational Approach for the Modeling/Decomposition
632 Strategy in the MINLP Optimization of Process Flowsheets with Implicit Models. *Ind. Eng. Chem.*
633 *Res.* 35, 2065–2070. <https://doi.org/10.1021/ie950424f>

634 Lastusilta, T., Bussieck, M., Emet, S., 2012. Extrinsic functions in GAMS. Presented at the
635 International Conference on Operations Research, Hannover.
636 <https://old.gams.com/presentations/or2012ef.pdf>

637 Malinen, I., 2011. Improving the robustness with modified bounded homotopies and problem-
638 tailored solving procedures (Ph. D.). University of Oulu, Oulu, Finlandia.

639 Manassaldi, J.I., 2017. Optimal synthesis and design of chemical processes involving discrete and
640 continuous decisions using mathematical programming (PhD Thesis). National Technological
641 University, Regional Faculty of Cordoba, Argentina.

642 Manassaldi, J.I., Arias, A.M., Scenna, N.J., Mussati, M.C., Mussati, S.F., 2016. A discrete and
643 continuous mathematical model for the optimal synthesis and design of dual pressure heat recovery
644 steam generators coupled to two steam turbines. *Energy* 103, 807–823.
645 <https://doi.org/10.1016/j.energy.2016.02.129>

646 Manassaldi, J.I., Mores, P.L., Scenna, N.J., Mussati, S.F., 2014. Optimal Design and Operating
647 Conditions of an Integrated Plant Using a Natural Gas Combined Cycle and Postcombustion CO₂
648 Capture. *Ind. Eng. Chem. Res.* 53, 17026–17042. <https://doi.org/10.1021/ie5004637>

649 Manassaldi, J.I., Mussati, M.C., Scenna, N.J., Mussati, S.F., 2018. User's manual to use
650 thermodynamic libraries in GAMS through extrinsic functions. GAMS.

651 Mazzei, M.S., Mussati, M.C., Mussati, S.F., 2014. NLP model-based optimal design of LiBr–H₂O
652 absorption refrigeration systems. *Int. J. Refrig.* 38, 58–70.
653 <https://doi.org/10.1016/j.ijrefrig.2013.10.012>

654 Mores, P.L., Manassaldi, J.I., Scenna, N.J., Caballero, J.A., Mussati, M.C., Mussati, S.F., 2018.
655 Optimization of the design, operating conditions, and coupling configuration of combined cycle
656 power plants and CO₂ capture processes by minimizing the mitigation cost. *Chem. Eng. J.* 331,
657 870–894. <https://doi.org/10.1016/j.cej.2017.08.111>

658 Mussati, S.F., Aguirre, P., Scenna, N., 2003a. Dual-purpose desalination plants. Part II. Optimal
659 configuration. *Desalination* 153, 185–189. [https://doi.org/10.1016/S0011-9164\(02\)01126-8](https://doi.org/10.1016/S0011-9164(02)01126-8)

660 Mussati, S.F., Aguirre, P., Scenna, N.J., 2001. Optimal MSF plant design. *Desalination, European
661 Conference on DESALINATION AND THE ENVIRONMENT WATER SHORTAGE* 138, 341–
662 347. [https://doi.org/10.1016/S0011-9164\(01\)00283-1](https://doi.org/10.1016/S0011-9164(01)00283-1)

663 Mussati, S.F., Aguirre, P.A., Scenna, N.J., 2005. Optimization of alternative structures of integrated
664 power and desalination plants. *Desalination, Desalination and the Environment* 182, 123–129.
665 <https://doi.org/10.1016/j.desal.2005.03.012>

666 Mussati, S.F., Aguirre, P.A., Scenna, N.J., 2004. A rigorous, mixed-integer, nonlinear programming
667 model (MINLP) for synthesis and optimal operation of cogeneration seawater desalination plants.
668 *Desalination, Desalination Strategies in South Mediterranean Countries* 166, 339–345.
669 <https://doi.org/10.1016/j.desal.2004.06.088>

670 Mussati, S.F., Aguirre, P.A., Scenna, N.J., 2003b. Novel Configuration for a Multistage Flash-
671 Mixer Desalination System. *Ind. Eng. Chem. Res.* 42, 4828–4839.
672 <https://doi.org/10.1021/ie020318v>

673 Mussati, S.F., Barttfeld, M., Aguirre, P.A., Scenna, N.J., 2008. A disjunctive programming model
674 for superstructure optimization of power and desalting plants. *Desalination* 222, 457–465.
675 <https://doi.org/10.1016/j.desal.2007.01.162>

676 Noronha, S., Gruhn, G., Kravanja, Z., 1997. Handling implicit model formulations in MINLP
677 optimization. *Comput. Chem. Eng., Supplement to Computers and Chemical Engineering* 21,
678 S499–S504. [https://doi.org/10.1016/S0098-1354\(97\)87551-5](https://doi.org/10.1016/S0098-1354(97)87551-5)

679 Onishi, V.C., Ravagnani, M.A.S.S., Jiménez, L., Caballero, J.A., 2017. Multi-objective synthesis of
680 work and heat exchange networks: Optimal balance between economic and environmental
681 performance. *Energy Convers. Manag.* 140, 192–202.
682 <https://doi.org/10.1016/j.enconman.2017.02.074>

683 Peng, D.-Y., Robinson, D.B., 1976. A New Two-Constant Equation of State. *Ind. Eng. Chem.
684 Fundam.* 15, 59–64. <https://doi.org/10.1021/i160057a011>

685 Poling, B.E., Prausnitz, J.M., O'Connell, J.P., 2001. *The Properties of Gases and Liquids*, 5th ed.
686 McGraw-Hill Education, New York.

687 Poth, N., Brusis, D., Stichlmair, J., 2003. Rigorous optimization of reactive distillation in GAMS
688 with the use of external functions, in: Kraslawski, A., Turunen, I. (Eds.), *Computer Aided Chemical
689 Engineering, European Symposium on Computer Aided Process Engineering-13*. Elsevier, pp. 869–
690 874. [https://doi.org/10.1016/S1570-7946\(03\)80226-2](https://doi.org/10.1016/S1570-7946(03)80226-2)

691 Recker, S., Skiborowski, M., Redepenning, C., Marquardt, W., 2015. A unifying framework for
692 optimization-based design of integrated reaction–separation processes. *Comput. Chem. Eng.,
693 Special Issue: Selected papers from the 8th International Symposium on the Foundations of*

694 Computer-Aided Process Design (FOCAPD 2014), July 13-17, 2014, Cle Elum, Washington, USA
695 81, 260–271. <https://doi.org/10.1016/j.compchemeng.2015.03.014>

696 Renon, H., Prausnitz, J.M., 1968. Local compositions in thermodynamic excess functions for liquid
697 mixtures. *AIChE J.* 14, 135–144. <https://doi.org/10.1002/aic.690140124>

698 Schilling, J., Gross, J., Bardow, A., 2017a. Integrated design of ORC process and working fluid
699 using process flowsheeting software and PC-SAFT. *Energy Procedia* 129, 129–136.
700 <https://doi.org/10.1016/j.egypro.2017.09.184>

701 Schilling, J., Tillmanns, D., Lampe, M., Hopp, M., Gross, J., Bardow, A., 2017b. Integrating
702 working fluid design into the thermo-economic design of ORC processes using PC-SAFT. *Energy*
703 *Procedia* 129, 121–128. <https://doi.org/10.1016/j.egypro.2017.09.179>

704 Skiborowski, M., Harwardt, A., Marquardt, W., 2015. Efficient optimization-based design for the
705 separation of heterogeneous azeotropic mixtures. *Comput. Chem. Eng., A Tribute to Ignacio E.*
706 *Grossmann* 72, 34–51. <https://doi.org/10.1016/j.compchemeng.2014.03.012>

707 Skiborowski, M., Recker, S., Marquardt, W., 2018. Shortcut-based optimization of distillation-
708 based processes by a novel reformulation of the feed angle method. *Chem. Eng. Res. Des.* 132,
709 135–148. <https://doi.org/10.1016/j.cherd.2018.01.019>

710 Skiborowski, M., Wessel, J., Marquardt, W., 2014. Efficient Optimization-Based Design of
711 Membrane-Assisted Distillation Processes. *Ind. Eng. Chem. Res.* 53, 15698–15717.
712 <https://doi.org/10.1021/ie502482b>

713 TDM-GCC, 2018. A compiler suite for 32- and 64-bit Windows based on the GNU toolchain.
714 <http://tdm-gcc.tdragon.net/> (accessed 7 January 2019).

715 Tolsma, J.E., Clabaugh, J.A., Barton, P.I., 2002. Symbolic Incorporation of External Procedures
716 into Process Modeling Environments. *Ind. Eng. Chem. Res.* 41, 3867–3876.
717 <https://doi.org/10.1021/ie0107946>

718 Tolsma, J.E., Clabaugh, J.A., Barton, P.I., 2000. ABACUSS II: Advanced Modeling Environment
719 and Embedded Process Simulator. Camb. MA. <http://yoric.mit.edu/abacuss2/abacuss2.html>

720 Waltermann, T., Skiborowski, M., 2016. Efficient optimization-based design of energetically
721 intensified distillation processes, in: Kravanja, Z., Bogataj, M. (Eds.), *Computer Aided Chemical*
722 *Engineering*, 26 European Symposium on Computer Aided Process Engineering. Elsevier, pp. 571–
723 576. <https://doi.org/10.1016/B978-0-444-63428-3.50100-4>

724 Yeomans, H., Grossmann, I.E., 2000. Disjunctive Programming Models for the Optimal Design of
725 Distillation Columns and Separation Sequences. *Ind. Eng. Chem. Res.* 39, 1637–1648.
726 <https://doi.org/10.1021/ie9906520>

727

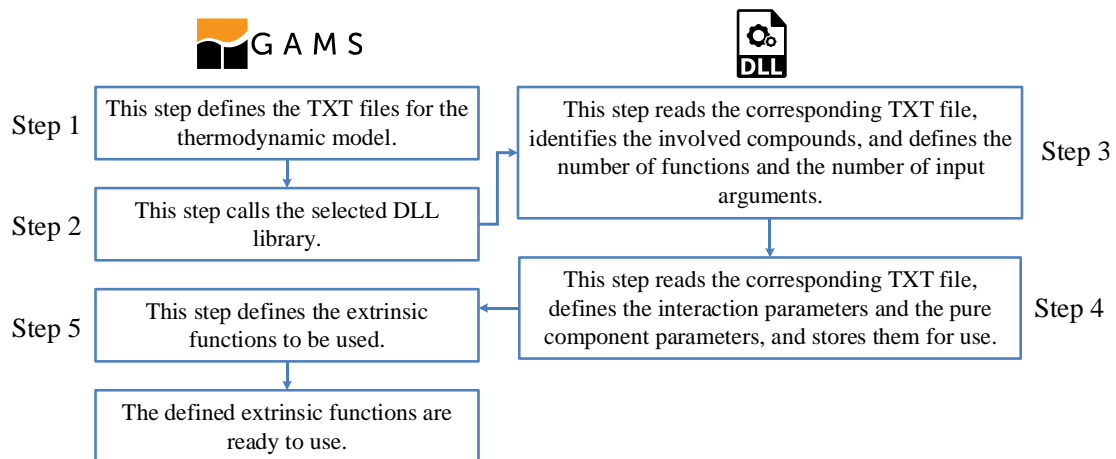


Figure 1. Steps of the DLL library loading process.

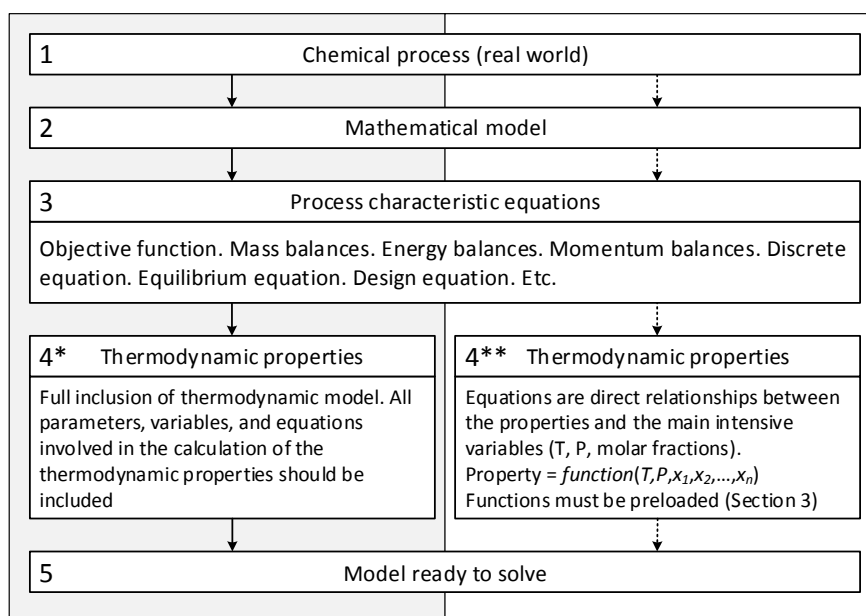


Figure 2. Classical strategy (solid line) and DLL-based strategy (dotted line) to build mathematical models in a AML software.

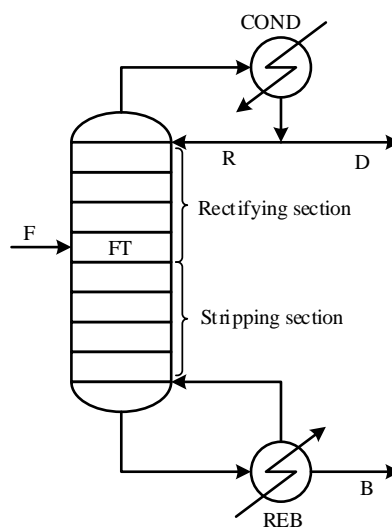


Figure 3. Schematic of a distillation column.

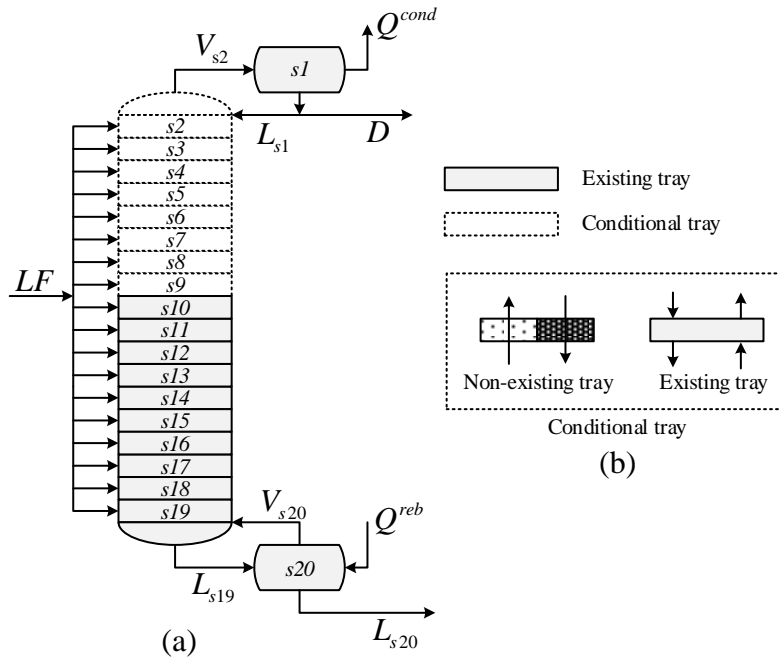


Figure 4. Schematics of (a) distillation column superstructure and (b) conditional tray approach, for modeling purpose.

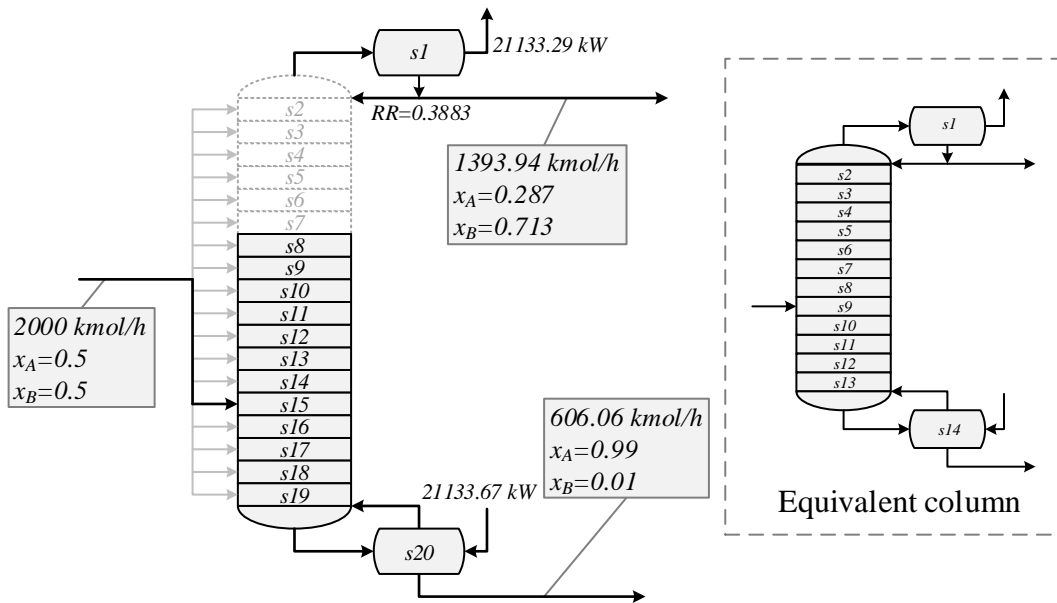


Figure 5. Optimal configuration of the distillation column obtained for the case study 1.

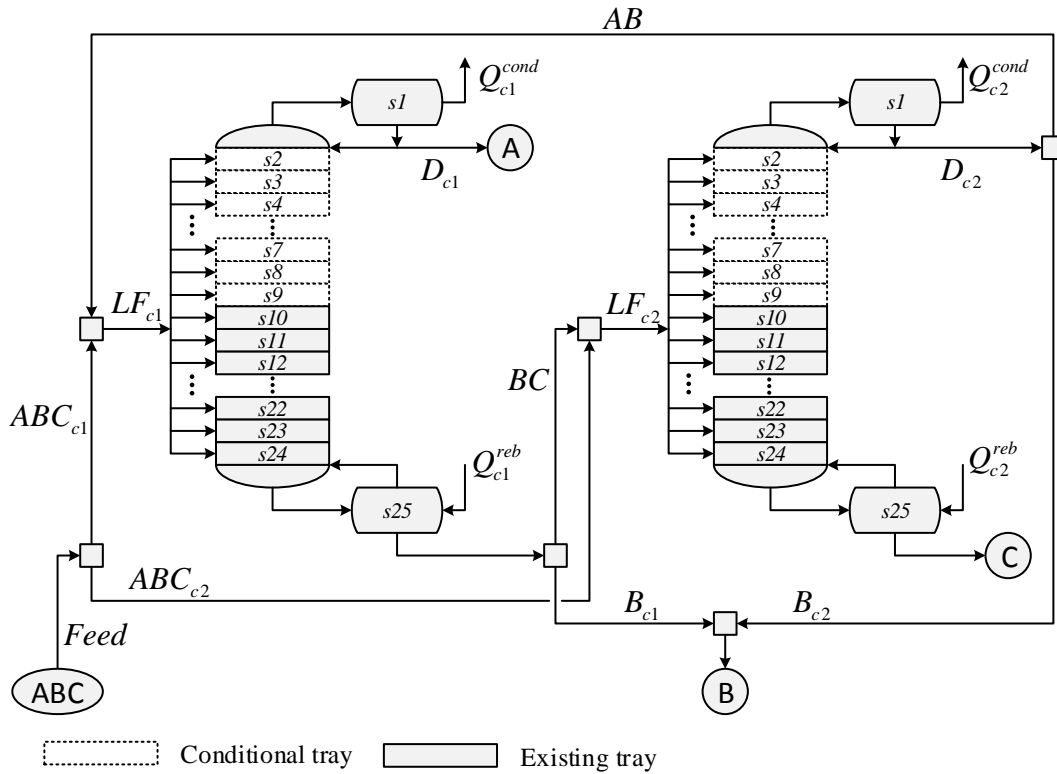


Figure 6. Schematic of a distillation sequence superstructure for a mixture of three components.

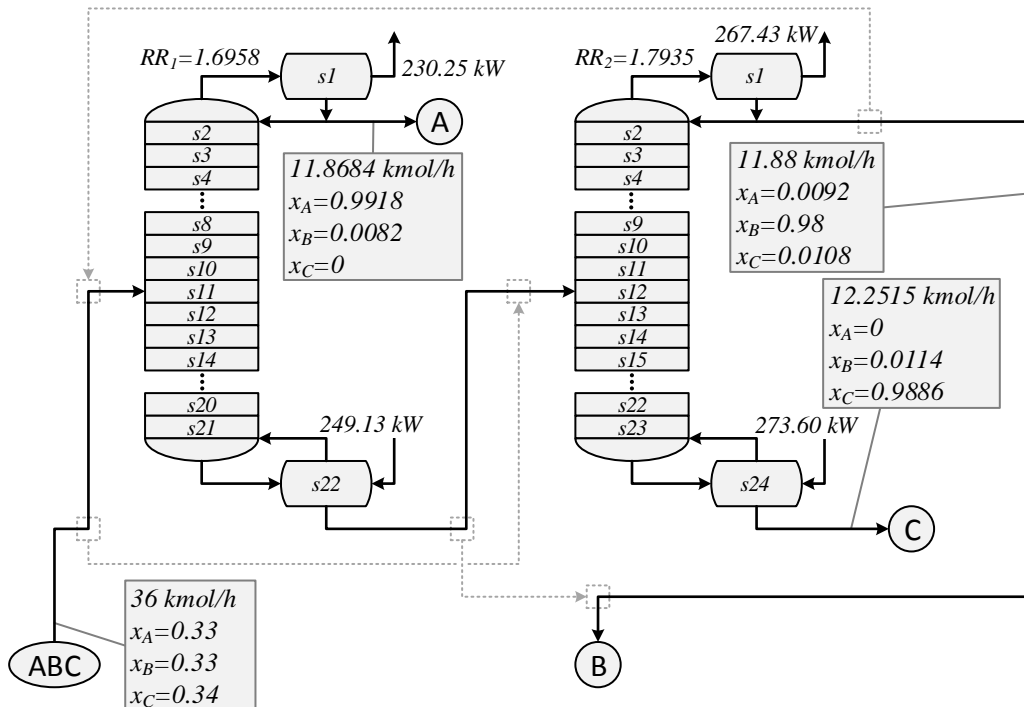


Figure 7. Optimal distillation sequence obtained for the case study 2.

Figure captions

Figure 1. Steps of the DLL library loading process.

Figure 2. Classical strategy (solid line) and DLL-based strategy (dotted line) to build mathematical models in a AML software.

Figure 3. Schematic of a distillation column.

Figure 4. Schematics of (a) distillation column superstructure and (b) conditional tray approach, for modeling purpose.

Figure 5. Optimal configuration of the distillation column obtained for the case study 1.

Figure 6. Schematic of a distillation sequence superstructure for a mixture of three components.

Figure 7. Optimal distillation sequence obtained for the case study 2.

Table 1. Extrinsic functions considered in each DLL library.

Property	Comments	Units
$\rho_{liq}(T, P, x_1, x_2, \dots, x_n)$	Density of the liquid phase	mol/m ³
$\rho_{vap}(T, P, x_1, x_2, \dots, x_n)$	Density of the vapor phase	mol/m ³
$h_{liq}(T, P, x_1, x_2, \dots, x_n)$	Enthalpy of the liquid phase	J/mol
$h_{vap}(T, P, x_1, x_2, \dots, x_n)$	Enthalpy of the vapor phase	J/mol
$s_{liq}(T, P, x_1, x_2, \dots, x_n)$	Entropy of the liquid phase	J/(mol·K)
$s_{vap}(T, P, x_1, x_2, \dots, x_n)$	Entropy of the vapor phase	J/(mol·K)
$fI_{liq}(T, P, x_1, x_2, \dots, x_n)$	Fugacity of component I in the liquid phase	bar
$fI_{vap}(T, P, x_1, x_2, \dots, x_n)$	Fugacity of component I in the vapor phase	bar
$f2_{liq}(T, P, x_1, x_2, \dots, x_n)$	Fugacity of component 2 in the liquid phase	bar
$f2_{vap}(T, P, x_1, x_2, \dots, x_n)$	Fugacity of component 2 in the vapor phase	bar
$fn_{liq}(T, P, x_1, x_2, \dots, x_n)$	Fugacity of component n in the liquid phase	bar
$fn_{vap}(T, P, x_1, x_2, \dots, x_n)$	Fugacity of component n in the vapor phase	bar

Table 2. Two implementation ways of the thermodynamic packages.

Classical approach (MS1)		DLL library-based strategy (MS2)	
$fug_{s,i}^l = \gamma_{s,i} x_{s,i} P_{s,i}^{sat} \text{poy}_{s,i}$	$\forall s; \forall i$ (24)	$fug_{s,i}^l = f_i^l(T_s^l, P_s, x_{s,A}, x_{s,B})$	$\forall s; \forall i$ (28)
$fug_{s,i}^v = y_{s,i} P$	$\forall s; \forall i$ (25)	$fug_{s,i}^v = f_i^v(T_s^v, P_s, y_{s,A}, y_{s,B})$	$\forall s; \forall i$ (29)
$H_s^l = \sum_{i=1}^n x_{s,i} (H_{s,i}^{l,IG} - \Delta H_{s,i}^{vap} + \Delta H_{s,i}^{ex})$	$\forall s$ (26)	$H_s^l = h^l(T_s^l, P_s, x_{s,A}, x_{s,B})$	$\forall s$ (30)
$H_s^v = \sum_{i=1}^n y_{s,i} H_{s,i}^{v,IG}$	$\forall s$ (27)	$H_s^v = h^v(T_s^v, P_s, y_{s,A}, y_{s,B})$	$\forall s$ (31)

Equations (B.1) to (B.22) (Appendix B)

Table 3. Optimization mathematical models considering both strategies (MS1 and MS2).

Classical strategy (MS1)	DLL library based strategy (MS2)
Minimize TAC	Minimize TAC
Subject to:	Subject to:
Eq.(1) to Eq.(23)	Eq.(1) to Eq.(23)
Eq.(24) to Eq.(27)	Eq.(28) to Eq.(31)
Eq.(B.1) to Eq.(B.22)	

Table 4. Model statistics of case study 1.

	Classical strategy (MS1)	DLL library based strategy (MS2)
Number of equations	1478	477
Continuous variables	1375	374
Discrete variables	8	8
Time for NLPs (s)	4.137	2.396
Number of iterations	826	1139
B&B nodes	16	16
TAC (\$/year)	2982000	2982000

Table 5. Deviation of average output values obtained by the GAMS model with DLL libraries (MS2) and process simulators.

	Temperature	Liquid flow	Vapor flow
ChemSep (ChemSep, 2018)	< 0.0008%	< 0.0002%	< 0.0002%
Hysys (Aspentech, 2018)	0.047%	0.364%	0.185%
Dwsim (Medeiros, 2018)	0.016%	0.493%	0.260%

Table 6. Model statistics of case study 2.

	Classical strategy (MS1)	DLL library-based strategy (MS2)
Number of equations	5910	1510
Continuous variables	5345	1145
Discrete variables	16	16
Time for NLPs (s)	410.813	193.348
Number of iterations	19120	34562
B&B nodes	160	160
TAC (\$/year)	153410	153410

Table 7. Performance comparison between external equations and extrinsic functions.

	External equations libraries (Aachener Verfahrenstechnik, 2019b).	Extrinsic function libraries (This work)
Total annual cost (€/year)	154647.6	158532.2
Number of equilibrium stages	70	72
Feed stage location	32	26
Column height (m)	38	39
Column diameter (m)	0.646	0.65
Resource usage (s)	4.57	0.219
Number of iterations	654	665
Single variable	1542	1542
Single equation	2104	2024
NLP solver	SNOPT 7.2-12.1	SNOPT 7.2-12.1

Table A.1. Methods for estimating thermodynamic properties in the DLL library corresponding to the NRTL model (*NRTLideal.dll*)

Function	Calculation method
<i>rho_liq</i>	Liquid mixture density by the Hankinson and Thomson method.
<i>rho_vap</i>	Ideal gas density
<i>h_liq</i>	Ideal liquid enthalpy plus excess enthalpy (from activity coefficient).
<i>h_vap</i>	Ideal gas enthalpy.
<i>s_liq</i>	Ideal liquid entropy plus excess entropy (from activity coefficient).
<i>s_vap</i>	Ideal gas entropy.
<i>f#_liq</i>	Liquid fugacity from activity coefficient (NRTL model) including the Poynting factor.
<i>f#_vap</i>	Ideal gas fugacity.

Table A.2. Methods for estimating thermodynamic properties in the DLL library corresponding to the Raoult's law (*RaoultLaw.dll*)

Function	Calculation method
<i>rho_liq</i>	Liquid mixture density by the Hankinson and Thomson method.
<i>rho_vap</i>	Ideal gas density.
<i>h_liq</i>	Ideal liquid enthalpy.
<i>h_vap</i>	Ideal gas enthalpy.
<i>s_liq</i>	Ideal liquid entropy.
<i>s_vap</i>	Ideal gas entropy.
<i>f#_liq</i>	Liquid fugacity considering unitary activity coefficient without including the Poynting factor.
<i>f#_vap</i>	Ideal gas fugacity.

Table A.3. Methods for estimating thermodynamic properties in the DLL library corresponding to the Peng-Robinson EOS (*PengRobinson.dll*)

Function	Calculation method
<i>rho_liq</i>	Liquid density estimated using the liquid phase compressibility factor.
<i>rho_vap</i>	Vapor density estimated using the vapor phase compressibility factor.
<i>h_liq</i>	Liquid enthalpy estimated using the ideal gas enthalpy and the liquid departure enthalpy.
<i>h_vap</i>	Vapor enthalpy estimated using the ideal gas enthalpy and the vapor departure enthalpy.
<i>s_liq</i>	Liquid entropy estimated using the ideal gas entropy and the liquid departure entropy.
<i>s_vap</i>	Vapor entropy estimated using the ideal gas entropy and the vapor departure entropy.
<i>f#_liq</i>	Liquid fugacity estimated using the liquid fugacity coefficient.
<i>f#_vap</i>	Vapor fugacity estimated using the vapor fugacity coefficient.

Table A.4. Thermodynamic property estimation methods for pure compounds.

Property	Estimation method
Ideal gas heat capacity	Reid-Prausnitz-Poling (RPP) fourth order polynomial.
Heat of vaporization	Using a temperature correlation obtained from the Chemsep database.
Vapor pressure	Using a temperature correlation obtained from the Chemsep database.
Saturated liquid volume	Hankinson and Thomson method.
Critical properties	Chemsep database.

Supplementary material

Development of Extrinsic Functions for Optimal Synthesis and Design—Application to Distillation-based Separation Processes

Juan I. Manassaldi^a, *Miguel C. Mussati*^{a,b}, *Nicolás J. Scenna*^a, *Sergio F. Mussati*^{a,b}

^a CAIMI Centro de Aplicaciones Informáticas y Modelado en Ingeniería (UTN-FRRo), Zeballos 1341, S2000BQA, Rosario, Argentina

^b INGAR Instituto de Desarrollo y Diseño (CONICET-UTN), Avellaneda 3657, S3002GJC, Santa Fe, Argentina

jmanassaldi@frro.utn.edu.ar, mmussati@santafe-conicet.gov.ar, nscenna@santafe-conicet.gov.ar, mussati@santafe-conicet.gov.ar

1. Introduction

This supplementary material provides to all the users the basic steps to use three general-purpose thermodynamic libraries in GAMS employing extrinsic functions.

- RaoultLaw.dll: Ideal solution (liquid phase) + Ideal gas (vapor phase).
- NRTLideal.dll: NRTL activity coefficient (liquid phase) + Ideal gas (vapor phase).
- PengRobinson.dll: Peng Robinson equation of state (both phases).

Below, general characteristics of the developed libraries are briefly summarized:

- Contain a database of 430 pure compounds.
- In a txt file, the IDs of the desired compounds and their interaction parameters (if necessary) should be defined.
- All functions have as input arguments the Temperature, Pressure and molar fraction of each mixture component. For example, for a binary mixture, the functions will have 4 input arguments.
- The input arguments of the function vary with the number of compounds involved.
- They support up to 18 compounds. Temperature + Pressure + 18 compounds = 20 argument (maximum arguments of extrinsic function for GAMS).
- All extrinsic functions have an analytic implementation of their gradient vector and Hessian matrix.
- Extrinsic Functions implemented in each library:
 - Liquid and vapor phase density.
 - Liquid and vapor phase enthalpy.
 - Liquid and vapor phase entropy.
 - Fugacity of each component in each phase (vapor and liquid).
- The database for pure compounds is taken from:

ChemSep v7.15 pure component data - Copyright (c) Harry Kooijman and Ross Taylor (2016) - http://www.perlfoundation.org/artistic_license_2_0

- The libraries were developed in *Dev C++* and using *tdm-gcc* as a compiler.
- More information about the library can be found in the compilation section of the *lst* file.

2. Basic steps required for configure and use the libraries

2.1. Compounds Assignment

Before including any of the libraries, the desired compounds must be assigned in a *txt* file. As shown in Table 1, each library has a defined file name.

Table 1. ID filename for each library

Library	ID file name
<i>RaoultLaw.dll</i>	<i>RaoultLawID.txt</i>
<i>PengRobinson.dll</i>	<i>PengRobinsonID.txt</i>
<i>NRTLideal.dll</i>	<i>NRTLidealID.txt</i>

Then, the compounds desired by the users are defined from their ID in the pure compounds database (ChemSep v7.15 pure component data - Copyright (c) Harry Kooijman and Ross Taylor). Appendix 1 presents a list including the available compounds with their corresponding IDs.

An illustrative example considering the Peng Robinson's equation of state and five compounds (propane, isobutane, n-butane, isopentane and n-pentane) is shown below:

```
$onecho > PengRobinsonID.txt
ID1 3
ID2 4
ID3 5
ID4 8
ID5 7
$offecho
```

As indicated, only one space should be used to separate the compound number and its database ID.

2.2. Interaction parameter definition

Depending on the selected thermodynamic package, it is necessary to define a group of interaction parameters. Again, each library has a file name assigned to each interaction group, as shown in Table 2.

Table 2. Interaction parameters file name for each library

Library	Interaction parameters file name	Units
<i>PengRobinson.dll</i>	<i>PengRobinsonaij.txt</i>	unitless
<i>NRTLideal.dll</i>	<i>NRTLidealaij.txt</i>	cal/mol
	<i>NRTLidealalphaij.txt</i>	unitless

Only binary interaction parameters that are not repeated should be defined. Interaction parameters declaration for the previously defined mixture is shown below.

```
$onecho > PengRobinsonaij.txt
a12 -0.0078
a13 0.0033
a14 0.0111
```

```
a15 0.0267
a23 -0.0004
a24 0.0005043
a25 0.00067951
a34 0.00021669
a35 0.0174
a45 0.06
$offecho
```

As example, the definition of parameters corresponding to a mixture consisting of ethanol and water using the *NRTLideal.dll* library is shown below.

```
$onecho > NRTLidealID.txt
ID1 1921
ID2 1102
$offecho
$onecho > NRTLidealaij.txt
a12 -57.9601
a21 1241.7396
$offecho
$onecho > NRTLidealalphaij.txt
alpha12 0.2937
$offecho
```

As shown (for *NRTLideal.dll*), the values of the parameters a_{12} and a_{21} must be defined because they are different. But, α_{12} and α_{21} have the same values. Therefore, α_{12} is only defined and then the library assigns internally the same values for α_{21} . In the current version, the dependence of the interaction parameters with the temperature is neglected. In future versions, this will be added to improve the NRTL library capabilities.

2.3. Including the developed libraries in GAMS

The following internal coding is used to include the libraries into GAMS:

```
$FuncLibIn <InternalLibName> <ExternalLibName>
```

For example, the *NRTLideal.dll* library is included as follows:

```
$FuncLibIn NRTLideal NRTLideal.dll
```

The *NRTLideal.dll* file must be placed in the subdirectory *gamsdir/projdir*, otherwise, the corresponding fullpath must be specified. The library must be included after the definition of the compounds and interaction parameters.

Once the library is included, the functions arguments are automatically assigned to specify temperature, pressure, and compositions. Thus, the total number of arguments required depends on the number of compounds. For instance, the arguments needed for a binary mixture are four (T , P , x_1 , x_2). In the compilation section in the *lst* file, it is possible to check if the compounds have been well identified. For example, the following information corresponds to *NRTLideal.dll* library execution (ethanol and water mixture).


```

FUNCLIBIN  NRTLideal  NRTLideal.dll
Function Library NRTLideal
NRTL + IG Property Package v0.9 by Ph.D. J.I. Manassaldi (jmanassaldi@frro.utn.edu.ar); Ph.D. N.J. Scenna; Ph.D. M.C. Mussati; Ph.D. S.F. Mussati (mussati@santafe-conicet.gov.ar)
GAMS Development Corporation

Mod. Function          Description
Type
NLP  rho_liq(temperature [k],pressure [bar],water,ethanol)liquid phase molar density [mol/m3]
NLP  rho_vap(temperature [k],pressure [bar],water,ethanol)vapor phase molar density [mol/m3]
NLP  h_liq(temperature [k],pressure [bar],water,ethanol)liquid phase molar enthalpy [J/mol]
NLP  h_vap(temperature [k],pressure [bar],water,ethanol)vapor phase molar enthalpy [J/mol]
NLP  s_liq(temperature [k],pressure [bar],water,ethanol)liquid phase molar entropy [J/(mol.K)]
NLP  s_vap(temperature [k],pressure [bar],water,ethanol)vapor phase molar entropy [J/(mol.K)]
NLP  f1_liq(temperature [k],pressure [bar],water,ethanol)liquid phase fugacity of component 1 [bar]
NLP  f1_vap(temperature [k],pressure [bar],water,ethanol)vapor phase fugacity of component 1 [bar]
NLP  f2_liq(temperature [k],pressure [bar],water,ethanol)liquid phase fugacity of component 2 [bar]
NLP  f2_vap(temperature [k],pressure [bar],water,ethanol)vapor phase fugacity of component 2 [bar]

```

To avoid inconsistencies, it is important to observe the units of the input and output arguments of the functions.

2.4. Functions definition

After the library is included, the necessary functions must be defined. This task is also done using an internal coding of GAMS, which is indicated below:

```
function <InternalFuncName> /<InternalLibName>.<FuncName>/;
```

Thus, by applying the above internal code, the function for *liquid enthalpy* corresponding to the *NRTLideal.dll* library is defined as follows:

```
function hliq /NRTLideal.h_liq/;
```

In this example, for convenience, the original extrinsic function *h_liq* was redefined (for GAMS code) as *hliq*.

Appendix 2 shows the definition of the libraries considered for the case studies presented in this work.

3. Usage of libraries

Once the previous steps have been completed, the developed extrinsic functions are already available for use. They can be used to define parameters or include them in an equation.

In this section, an illustrative optimization example to show a detailed application of one of the developed libraries (*NRTLideal.dll*) is presented.

The objective of the optimization problem is to calculate the composition and temperature of a binary minimum-boiling homogeneous azeotrope. Precisely, a water-ethanol mixture is considered and the pressure is fixed at 1.0132 bar.

To do this, the following GAMS model has been used:

```

$onecho > NRTLidealID.txt
ID1 1921
ID2 1102
$offecho
$onecho > NRTLidealaij.txt
a12 1241.7396
a21 -57.9601
$offecho
$onecho > NRTLidealalphaij.txt
alpha12 0.2937
$offecho
$funclibin NRTLideal NRTLideal.dll
function f1l /NRTLideal.f1_liq /;
function f2l /NRTLideal.f2_liq /;
function f1v /NRTLideal.f1_vap /;
function f2v /NRTLideal.f2_vap /;

sets
i compounds /water,ethanol/
;
Parameter
P pressure [bar] /1.0132/
;
Variable
T temperature [K]
x(i) liquid molar fraction
y(i) vapor molar fraction
;
equation
eq1,eq2 phase equilibrium equations
eq3,eq4 sumatory of component molar fractions
;
eq1.. f1l(T,P,x('water'),x('ethanol')) =e= f1v(T,P,y('water'),y('ethanol'));
eq2.. f2l(T,P,x('water'),x('ethanol')) =e= f2v(T,P,y('water'),y('ethanol'));
eq3.. sum(i,y(i)) =e= 1;
eq4.. sum(i,x(i)) =e= 1;

y.lo(i)=0; y.up(i)=1;
x.lo(i)=0; x.up(i)=1;

y.l(i)=0.5;
x.l(i)=0.5;
T.l=350;

model azeotrope /all/;
solve azeotrope using nlp minimizing T;

```

The obtained results are compared (Table 3) with experimental data taken from Tochigi et al. (1985). Despite the assumptions made to derive the model, for instance, the dependence of the NRTL interaction parameters with the temperature is neglected, a good agreement between the predicted and experimental results is observed.

Table 3. Comparison of the model-based results and experimental value (1.0132 bar)

	GAMS model	Experimental data ^(*)
Temperature [K]	351.5302	351.34
Composition (ethanol molar fraction)	0.8681	0.894

^(*) Tochigi, K., Inoue, H., and Kojima, K. (1985). Determination of azeotropes in binary systems at reduced pressures. Fluid Phase Equilibria 22, 343–352.

Appendix 1. Supported compounds with the corresponding IDs.

ID	Name	ID	Name	ID	Name
1	Methane	505	O-xylene	1319	Isopropyl acetate
2	Ethane	506	M-xylene	1321	Vinyl acetate
3	Propane	507	P-xylene	1322	Methyl propionate
4	Isobutane	509	N-propylbenzene	1351	Methyl methacrylate
5	N-butane	510	Cumene	1357	N-pentyl acetate
7	N-pentane	511	O-ethyltoluene	1363	N-hexyl acetate
8	Isopentane	512	M-ethyltoluene	1366	Ethylene carbonate
9	Neopentane	513	P-ethyltoluene	1381	Dimethyl terephthalate
11	N-hexane	514	1,2,3-trimethylbenzene	1401	Dimethyl ether
12	2-methylpentane	515	1,2,4-trimethylbenzene	1402	Diethyl ether
13	3-methylpentane	516	Mesitylene	1403	Diisopropyl ether
14	2,2-dimethylbutane	518	N-butylbenzene	1404	Di-n-butyl ether
15	2,3-dimethylbutane	519	Isobutylbenzene	1405	Methyl tert-butyl ether
17	N-heptane	520	Sec-butylbenzene	1406	Di-sec-butyl ether
18	2-methylhexane	521	Tert-butylbenzene	1407	Methyl ethyl ether
19	3-methylhexane	522	O-cymene	1408	Methyl n-propyl ether
20	3-ethylpentane	523	M-cymene	1409	Isopropyl butyl ether
21	2,2-dimethylpentane	524	P-cymene	1410	Methyl isobutyl ether
22	2,3-dimethylpentane	525	O-diethylbenzene	1411	Methyl isopropyl ether
23	2,4-dimethylpentane	526	M-diethylbenzene	1421	1,4-dioxane
24	3,3-dimethylpentane	527	P-diethylbenzene	1427	Methyl tert-pentyl ether
25	2,2,3-trimethylbutane	530	1,2,3,4-tetramethylbenzene	1428	Tert-butyl ethyl ether
27	N-octane	531	1,2,3,5-tetramethylbenzene	1430	Ethyl tert-pentyl ether
28	2-methylheptane	532	1,2,4,5-tetramethylbenzene	1431	Methylal
29	3-methylheptane	544	P-diisopropylbenzene	1441	Ethylene oxide
30	4-methylheptane	558	Biphenyl	1442	1,2-propylene oxide
31	3-ethylhexane	576	2-ethyl-m-xylene	1447	Butyl vinyl ether
32	2,2-dimethylhexane	577	2-ethyl-p-xylene	1461	Anisole
33	2,3-dimethylhexane	578	4-ethyl-m-xylene	1472	Cumene hydroperoxide
34	2,4-dimethylhexane	579	4-ethyl-o-xylene	1479	Tetrahydrofuran
35	2,5-dimethylhexane	586	1-methyl-3-n-propylbenzene	1501	Carbon tetrachloride
36	3,3-dimethylhexane	587	1-methyl-4-n-propylbenzene	1502	Methyl chloride
37	3,4-dimethylhexane	601	Styrene	1503	Ethyl chloride
38	2-methyl-3-ethylpentane	701	Naphthalene	1504	Vinyl chloride

39	3-methyl-3-ethylpentane	702	1-methylnaphthalene	1521	Chloroform
40	2,2,3-trimethylpentane	703	2-methylnaphthalene	1522	1,1-dichloroethane
41	2,2,4-trimethylpentane	710	1-phenylnaphthalene	1523	1,2-dichloroethane
42	2,3,3-trimethylpentane	717	Fluoranthene	1524	1,1,2-trichloroethane
43	2,3,4-trimethylpentane	723	1-methylindene	1541	Trichloroethylene
44	2,2,3,3-tetramethylbutane	724	2-methylindene	1571	Monochlorobenzene
46	N-nonane	738	Fluorene	1572	O-dichlorobenzene
47	2,2,5-trimethylhexane	803	Indene	1573	M-dichlorobenzene
48	3,3,5-trimethylheptane	805	Phenanthrene	1574	P-dichlorobenzene
49	2,4,4-trimethylhexane	806	Chrysene	1592	1,2,4-trichlorobenzene
50	3,3-diethylpentane	807	Pyrene	1680	Bromobenzene
51	2,2,3,3-tetramethylpentane	808	Acenaphthene	1681	Methyl iodide
52	2,2,3,4-tetramethylpentane	820	Indane	1691	Iodobenzene
53	2,2,4,4-tetramethylpentane	899	Nitrous oxide	1701	Methylamine
54	2,3,3,4-tetramethylpentane	900	Nitrogen dioxide	1703	Trimethylamine
55	Squalane	901	Oxygen	1704	Ethylamine
56	N-decane	902	Hydrogen	1706	Triethylamine
62	Tert-butylcyclohexane	904	Nitrogen trioxide	1710	Diethylamine
63	N-undecane	905	Nitrogen	1722	Methyl DiEthanolAmine
64	N-dodecane	906	Nitrogen tetroxide	1723	Monoethanolamine
65	N-tridecane	908	Carbon monoxide	1724	Diethanolamine
66	N-tetradecane	909	Carbon dioxide	1725	Triethanolamine
67	N-pentadecane	910	Sulfur dioxide	1741	Ethylenediamine
68	N-hexadecane	911	Sulfur trioxide	1743	Diisopropylamine
69	N-heptadecane	912	Nitric oxide	1750	N-aminoethyl piperazine
70	N-octadecane	913	Helium-4	1760	Nitromethane
71	N-nonadecane	914	Argon	1761	Nitroethane
72	2,2-dimethyloctane	915	Air	1762	1-nitropropane
73	N-eicosane	917	Fluorine	1763	2-nitropropane
74	N-heneicosane	918	Chlorine	1769	1-nitrobutane
75	N-docosane	919	Neon	1771	Hydrogen cyanide
76	N-tricosane	920	Krypton	1772	Acetonitrile
77	N-tetracosane	922	Bromine	1773	Propionitrile
78	N-pentacosane	924	Ozone	1774	Acrylonitrile
79	N-hexacosane	959	Xenon	1775	Methacrylonitrile
80	N-heptacosane	1001	Formaldehyde	1778	O-nitrotoluene
81	N-octacosane	1002	Acetaldehyde	1779	P-nitrotoluene
82	N-nonacosane	1003	Propanal	1780	M-nitrotoluene
85	3-methylnonane	1005	Butanal	1791	Pyridine
86	2-methylnonane	1006	2-methylpropanal	1792	Aniline
87	4-methylnonane	1007	Pentanal	1801	Methyl mercaptan
88	5-methylnonane	1008	Heptanal	1802	Ethyl mercaptan
91	2-methyloctane	1009	Hexanal	1803	N-propyl mercaptan
92	3-methyloctane	1051	Acetone	1804	Tert-butyl mercaptan

93	4-methyloctane	1052	Methyl ethyl ketone	1805	Isobutyl mercaptan
94	3-ethylheptane	1053	3-pentanone	1806	Sec-butyl mercaptan
96	2,2-dimethylheptane	1054	Methyl isobutyl ketone	1807	N-hexyl mercaptan
102	Cyclobutane	1057	3-heptanone	1810	Isopropyl mercaptan
104	Cyclopentane	1058	4-heptanone	1813	Methyl ethyl sulfide
105	Methylcyclopentane	1059	3-hexanone	1814	Methyl n-propyl sulfide
107	Ethylcyclopentane	1060	2-pentanone	1815	Methyl t-butyl sulfide
108	1,1-dimethylcyclopentane	1061	Methyl isopropyl ketone	1816	Methyl t-pentyl sulfide
109	Cis-1,2-dimethylcyclopentane	1062	2-hexanone	1817	Di-n-propyl sulfide
110	Trans-1,2-dimethylcyclopentane	1063	2-heptanone	1818	Diethyl sulfide
111	Cis-1,3-dimethylcyclopentane	1064	5-methyl-2-hexanone	1820	Dimethyl sulfide
112	Trans-1,3-dimethylcyclopentane	1066	3,3-dimethyl-2-butanone	1821	Thiophene
114	N-propylcyclopentane	1068	Diisobutyl ketone	1824	Diethyl disulfide
115	Isopropylcyclopentane	1069	Diisopropyl ketone	1828	Dimethyl disulfide
116	1-methyl-1-ethylcyclopentane	1080	Cyclohexanone	1829	Di-n-propyl disulfide
122	N-butylcyclopentane	1100	Ketene	1844	Dimethyl sulfoxide
137	Cyclohexane	1101	Methanol	1845	Sulfolane
138	Methylcyclohexane	1102	Ethanol	1851	Acetyl chloride
140	Ethylcyclohexane	1103	1-propanol	1854	Dichloroacetyl chloride
141	1,1-dimethylcyclohexane	1104	Isopropanol	1855	Trichloroacetyl chloride
142	Cis-1,2-dimethylcyclohexane	1105	1-butanol	1876	N,n-dimethylformamide
143	Trans-1,2-dimethylcyclohexane	1106	2-methyl-1-propanol	1886	Nitrobenzene
144	Cis-1,3-dimethylcyclohexane	1107	2-butanol	1889	Furfural
145	Trans-1,3-dimethylcyclohexane	1108	2-methyl-2-propanol	1893	Carbonyl sulfide
146	Cis-1,4-dimethylcyclohexane	1109	1-pentanol	1894	Phosgene
147	Trans-1,4-dimethylcyclohexane	1110	2-pentanol	1903	Nitric acid
149	N-propylcyclohexane	1111	2-methyl-2-butanol	1904	Hydrogen chloride
152	N-butylcyclohexane	1112	2-methyl-1-butanol	1907	Hydrogen iodide
153	Cis-decahydronaphthalene	1113	2,2-dimethyl-1-propanol	1911	Ammonia
154	Trans-decahydronaphthalene	1114	1-hexanol	1921	Water
201	Ethylene	1125	1-heptanol	1922	Hydrogen sulfide
202	Propylene	1151	Cyclohexanol	1938	Carbon disulfide
204	1-butene	1181	Phenol	1940	Sulfur hexafluoride
205	Cis-2-butene	1182	O-cresol	2252	2-methyl-1-heptene
206	Trans-2-butene	1183	M-cresol	2367	Propylene carbonate
207	Isobutene	1184	P-cresol	2391	Dimethyl carbonate
209	1-pentene	1201	Ethylene glycol	2717	Diethylenetriamine
210	Cis-2-pentene	1202	Diethylene glycol	2732	N-aminoethyl ethanolamine
211	Trans-2-pentene	1203	Triethylene glycol	2743	2,4-dinitrotoluene
212	2-methyl-1-butene	1204	Tetraethylene glycol	2744	2,6-dinitrotoluene
213	3-methyl-1-butene	1231	Glycerol	2745	3,4-dinitrotoluene
214	2-methyl-2-butene	1241	1,4-butanediol	2747	2,4,6-trinitrotoluene
216	1-hexene	1252	Acetic acid	2748	2,5-dinitrotoluene
217	Cis-2-hexene	1253	Propionic acid	2749	3,5-dinitrotoluene

218	Trans-2-hexene	1255	Oxalic acid	2750	P-phenylenediamine
221	2-methyl-1-pentene	1256	N-butyric acid	2752	Piperazine
227	4-methyl-cis-2-pentene	1277	Acrylic acid	2856	N,n-dimethylacetamide
228	4-methyl-trans-2-pentene	1278	Methacrylic acid	3801	Di-tert-butyl disulfide
234	1-heptene	1281	Benzoic acid	3813	Ethyl methyl disulfide
250	1-octene	1282	O-toluic acid	3814	Ethyl propyl disulfide
259	1-nonene	1283	P-toluic acid	3819	Diphenyl disulfide
261	1-undecene	1284	Salicylic acid	4865	Trichloroacetaldehyde
270	Cyclohexene	1285	Adipic acid	4868	Dichloroacetaldehyde
301	Propadiene	1286	Maleic acid	6861	Diethylethanolamine
302	1,2-butadiene	1287	Phthalic acid	6862	Methylethanolamine
303	1,3-butadiene	1289	Terephthalic acid	6863	Dimethylethanolamine
309	Isoprene	1291	Acetic anhydride	6864	Diisopropanolamine
316	Dicyclopentadiene	1298	Maleic anhydride	13125	DiPhenyl Carbonate
401	Acetylene	1301	Methyl formate	20101	2-Methyl-2-Heptanol
402	Methylacetylene	1302	Ethyl formate	22158	2-Methoxy-2-Methyl-Heptane
403	Ethylacetylene	1303	N-propyl formate	22587	Ethyl Phenyl Carbonate
404	Dimethylacetylene	1312	Methyl acetate	23498	Methyl Ethyl Carbonate
418	Vinylacetylene	1313	Ethyl acetate	27991	Methyl Phenyl Carbonate
501	Benzene	1314	N-propyl acetate	28366	DiEthyl Carbonate
502	Toluene	1315	N-butyl acetate		
504	Ethylbenzene	1316	Isobutyl acetate		

Appendix 2. Library definition for the presented case studies

Case study 1 involves a mixture of water and ethanol. As shown in Appendix 1, the compounds IDs are 1921 and 1102 respectively.

```

$onecho > NRTLidealID.txt
ID1 1921
ID2 1102
$offecho
$onecho > NRTLidealaij.txt
a12 1241.7396
a21 -57.9601
$offecho
$onecho > NRTLidealalphaij.txt
alpha12 0.2937
$offecho
$funclibin NRTL NRTLideal.dll
function h_liq /NRTL.h_liq /;
function f1_liq /NRTL.f1_liq /;
function f2_liq /NRTL.f2_liq /;
function h_vap /NRTL.h_vap /;
function rho_vap /NRTL.rho_vap/;
function f1_vap /NRTL.f1_vap /;
function f2_vap /NRTL.f2_vap /;

```

In case study 2, a mixture of n-pentane, n-hexane and n-heptane is analyzed and the compounds IDs are 7, 11 and 17 respectively.

```
$onecho > PengRobinsonID.txt
ID1 7
ID2 11
ID3 17
$offecho
$onecho > PengRobinsonaij.txt
a12 0.000393
a13 0.001373
a23 0.000297
$offecho
$funclibin PengRobinson PengRobinson.dll
function h_liq /PengRobinson.h_liq /;
function f1_liq /PengRobinson.f1_liq /;
function f2_liq /PengRobinson.f2_liq /;
function f3_liq /PengRobinson.f3_liq /;
function h_vap /PengRobinson.h_vap /;
function rho_vap /PengRobinson.rho_vap/;
function f1_vap /PengRobinson.f1_vap /;
function f2_vap /PengRobinson.f2_vap /;
function f3_vap /PengRobinson.f3_vap /;
```

Finally, in the comparison example (Section 3.5), a mixture of methanol and ethanol is used. According to Appendix 1, the compounds IDs are 1101 and 1102 respectively.

```
$onecho > NRTLidealID.txt
ID1 1101
ID2 1102
$offecho
$onecho > NRTLidealaij.txt
a12 -327.9991
a21 376.2667
$offecho
$onecho > NRTLidealalphaij.txt
alpha12 0.3057
$offecho
$funclibin NRTL NRTLideal.dll
function f1_liq /NRTL.f1_liq /;
function f2_liq /NRTL.f2_liq /;
function f1_vap /NRTL.f1_vap /;
function f2_vap /NRTL.f2_vap /;
function h_liq /NRTL.h_liq /;
function h_vap /NRTL.h_vap /;
```

As mentioned in the manuscript, the gradient vector and the Hessian matrix were implemented analytically in each extrinsic function in the C programming language. As illustration, extracts of the source codes for computing the gradient vector and Hessian matrix in the extrinsic function corresponding to the liquid enthalpy in the Peng-Robinson library (*PengRobinson.dll*) are presented in Figs. S1 and S2, respectively.

```

167 | dHgdT = dHgdT + y[i]*dhididT[i]*1e-3;
168 | };
169 |
170 | double daux4dP = dzdP + dBpdP*(1+sqrt(2));
171 | double daux5dP = dzdP + dBpdP*(1-sqrt(2));
172 | double df3dP = daux4dP/aux4 - daux5dP/aux5;
173 | double ddepartureHdP = Rg*T*dzdP - f1*f2*df3dP;
174 |
175 | double dHgdY[i];
176 | for(i=0;i<ci;i+=1){
177 | dHgdY[i] = hidi[i]*1e-3;
178 | };
179 |
180 | double damdTy[ci];
181 | for(i=0;i<ci;i+=1){
182 | damdTy[i]=0;
183 | for(j=0;j<ci;j+=1){
184 | damdTy[i] = damdTy[i] + 2*y[j]*daijdT[j][i];
185 | };}
186 | double daux4dy[ci];
187 | double daux5dy[ci];
188 | double df1dy[ci];
189 | double df2dy[ci];
190 | double df3dy[ci];
191 | double ddepartureHdy[ci];
192 |
193 | for(i=0;i<ci;i+=1){
194 | daux4dy[i] = dzdy[i] + dBpdy[i]*(1+sqrt(2));
195 | daux5dy[i] = dzdy[i] + dBpdy[i]*(1-sqrt(2));
196 | df1dy[i] = damdy[i] - damdTy[i]*T;
197 | df2dy[i] = -dbmdy[i]/(2*sqrt(2)*pow(bm,2));
198 | df3dy[i] = daux4dy[i]/aux4 - daux5dy[i]/aux5;
199 | ddepartureHdy[i] = Rg*T*dzdy[i] - df1dy[i]*f2*f3 - f1*df2dy[i]*f3 - f1*f2*df3dy[i];
200 | };
201 |
202 | gradient[0] = dHgdT + ddepartureHdT; //dh/dT
203 | gradient[1] = ddepartureHdP; //dh/dP
204 | for(i=0;i<ci;i+=1){
205 | gradient[2+i] = dHgdY[i] + ddepartureHdy[i]; //dh/dyi
206 | };
207 |

```

Figure S1. Extract of the source code for computing the gradient vector corresponding to the liquid enthalpy in the Peng-Robinson library

In Fig. S1, the dotted box indicates how each position of the gradient vector of the enthalpy is calculated. The first position (gradient [0]) corresponds to the function derivative with respect to the first argument (temperature), the second position (gradient [1]) refers to the function derivative with respect to the second argument (pressure), and the third and successive positions refer to the function derivatives with respect to the third and successive arguments (concentration of each component).

Analogously, Fig. S2 shows the piece of source code corresponding to the computation of the Hessian matrix for the same example.


```

278 ddepartureHdPy[i] = Rg*T*dzdPy[i] - df1dy[i]*f2*df3dP - f1*df2dy[i]*df3dP - f1*f2*df3dPy[i];
279 };
280
281 double damdTyy[ci][ci];
282 double daux4dyy[ci][ci];
283 double daux5dyy[ci][ci];
284 double df1dyy[ci][ci];
285 double df2dyy[ci][ci];
286 double df3dyy[ci][ci];
287 double ddepartureHdyy[ci][ci];
288 for(j=0;j<ci;j+=1){
289 for(i=0;i<ci;i+=1){
290 damdTyy[i][j] = daijdT[i][j] + daijdT[j][i];
291 daux4dyy[i][j] = dzdyy[i][j];
292 daux5dyy[i][j] = dzdyy[i][j];
293 df1dyy[i][j] = damdyy[i][j] - damdTyy[i][j]*T;
294 df2dyy[i][j] = 2*dbmdy[i]*dbmdy[j]/(2*sqrt(2)*pow(bm,3));
295 df3dyy[i][j] = daux4dyy[i][j]/aux4 - daux4dy[i]*daux4dy[j]/pow(aux4,2) - daux5dyy[i][j]/au:
296 ddepartureHdyy[i][j] = Rg*T*dzdyy[i][j] - df1dyy[i][j]*f2*f3 - df1dy[i]*df2dy[j]*f3 - df1dy[
297 };};
298
299
300 hessian[0]= dHgdTT + ddepartureHdTT; //dh/dTdT
301 hessian[1]= ddepartureHdTP; //dh/dTdP
302 for(i=0;i<ci;i+=1){
303 hessian[2+i] = dHgdTy[i] + ddepartureHdTy[i]; //dh/dTdyi
304 };
305 hessian[2+ci] = ddepartureHdTP; //dh/dPdT
306 hessian[2+ci+1] = ddepartureHdPP; //dh/dPdP
307 for(i=0;i<ci;i+=1){
308 hessian[2+ci+2+i] = ddepartureHdPy[i]; //dh/dPdyi
309 };
310 int j;
311 for(i=0;i<ci;i+=1){
312 hessian[(2+i)*(2+ci)] = dHgdTy[i] + ddepartureHdTy[i]; //dh/dyidT
313 hessian[(2+i)*(2+ci)+1] = ddepartureHdPy[i]; //dh/dyidP
314 for(j=0;j<ci;j+=1){
315 hessian[(2+i)*(2+ci)+2+j] = ddepartureHdyy[i][j]; //dh/dyidyj
316 };
317 };

```

Figure S2. Extract of the source code for computing the Hessian matrix corresponding to the liquid enthalpy in the Peng-Robinson library.